eprints@whiterose.ac.uk
https://eprints.whiterose.ac.uk/

STATIC AXIALLY SYMMETRIC SOLUTIONS OF EINSTEIN-YANG-MILLS EQUATIONS WITH A NEGATIVE COSMOLOGICAL CONSTANT: BLACK HOLE SOLUTIONS

Eugen Radu[1] and Elizabeth Winstanley[2]

[1] *Department of Mathematical Physics, National University of Ireland, Maynooth, Ireland*
[2] *Department of Applied Mathematics, The University of Sheffield, Hicks Building,
Hounsfield Road, Sheffield, S3 7RH, United Kingdom.*

Abstract

We investigate static axially symmetric black hole solutions in a four-dimensional Einstein-Yang-Mills-SU(2) theory with a negative cosmological constant Λ. These solutions approach asymptotically the anti-de Sitter spacetime and possess a regular event horizon. A discussion of the main properties of the solutions and the differences with respect to the asymptotically flat case is presented. The mass of these configurations is computed by using a counterterm method. We note that the $\Lambda = -3$ configurations have an higher dimensional interpretation in context of $d = 11$ supergravity. The existence of axially symmetric monopole and dyon solutions in a fixed Schwarzschild-anti-de Sitter background is also discussed. An exact solution of the Einstein-Yang-Mills equations is presented in Appendix.

1   INTRODUCTION

There has been much interest in recent years in the study of black hole solutions in gravitational theories with a negative cosmological constant Λ. The initial interest in asymptotically anti-de Sitter (AAdS) solutions was due to the result that (sufficiently large) Schwarzschild-AdS (SAdS) black holes are thermodynamically stable [1]. A renewed interest in the study of AAdS black holes has appeared following the AdS/conformal field theory conjecture, which proposes a correspondence between physical effects associated with gravitating fields propagating in AdS spacetime and those of a conformal field theory (CFT) on the boundary of AdS spacetime [2, 3]. The AAdS black hole solutions would offer the posibility of studying the nonperturbative structure of some conformal field theories. For example, the AdS$_5$ Hawking-Page phase transition [1] is interpreted as a thermal phase transition from a confining to a deconfining phase in the dual $D = 4$, $N = 4$ super Yang-Mills theory [4], while the phase structure of Reissner- Nordström-AdS black holes resembles that of a van der Waals-Maxwell liquid-gas system [5]. Also, when $\Lambda < 0$, the so-called topological black holes, whose topology of the event horizon is no longer the two-sphere S^2 may appear (see [6] for reviews of the subject).

These results motivate at least partially attempts to find new black hole solutions in AAdS spacetimes. Particularly interesting are solutions violating the no hair conjecture. This conjecture states that the only allowed characteristics of a stationary black hole are those associated with the Gauss law, such as mass angular momentum and U(1) charge. Black holes with hair may be useful for probing not only quantum gravity, but also may be interesting tests of the AdS/CFT correspondence, particularly since we can find such objects which are classically stable. For AAdS black holes, it has been shown recently that conformally coupled scalar field can be painted as hair [7]. The existence of long range Nielson-Olesen vortex as hair for asymptotically AdS black holes has been investigated in [8, 9] for SAdS black hole and charged black strings.

AAdS black holes solutions with SU(2) nonabelian fields have been presented in [10, 11]. The obtained results are strikingly different from those valid in the asymptotically flat case (nontrivial solutions exist for all values of $\Lambda < 0$). For example, regular black hole solutions exist for continuous intervals of the parameter space, rather than discrete points and there are configurations for which the gauge field has no

---

zeros. Regular and black hole dyon solutions without a Higgs field have also been found [11]. Insofar as the no-hair theorem is concerned, it has been shown that there exist stable black hole solutions in SU(2) Einstein-Yang-Mills (EYM) theory that are AAdS [10, 11]. However, the same system in the presence of a Higgs scalar field presents only configurations with very similar properties to the asymptotically-flat space counterparts [12, 13, 14].

The literature on AAdS solutions with nonabelian fields is continuously growing, including stability analyses [15, 16], the study of configurations with a NUT charge [17], higher dimensional counterparts [18] and axially symmetric generalizations [19, 20]. Here we remark that the EYM black hole solutions with $\Lambda < 0$ discussed in the literature are spherically symmetric or correspond to topological black holes [21] presenting the same amount of symmetry. However, for a vanishing cosmological constant, the EYM-SU(2) theory is known to possess also static axially symmetric finite energy black hole solutions, as exhaustively discussed in [22, 23]. The situation for a nonabelian field is very different from the Einstein-Maxwell theory, where the static black hole solution is spherically symmetric. Representing generalizations of the well known spherically symmetric asymptotically flat black hole solutions [24], these static axially symmetric solutions are characterized by two integers, for a given event event horizon radius. These are the node number k of the gauge field functions and the winding number n with respect to the azimuthal angle φ . The static spherically symmetric solutions have winding number $n = 1$. Similar to the case of regular configurations [25], winding numbers $n > 1$ leads to axially symmetric black hole solutions. Outside their regular event horizon, the static $\Lambda = 0$ axially symmetric black hole solutions possess non-trivial magnetic gauge field configurations, but they carry no global magnetic charge. In a remarkable development, these asymptotically flat black hole solutions have been generalized to include the effects of rotation, leading to nonabelian counterparts of the Kerr-Newmann solution [26].

The regular $n > 1$ axially symmetric EYM configurations of Ref. [25] have been generalized for $\Lambda < 0$ in Ref. [20]. Although some common features are present, the results in the AAdS case are rather different from those valid in the $\Lambda = 0$ limit, in particular presenting arbitrary values for the mass and magnetic charge. These distinctions arise from differences that already exist in the spherically symmetric case.

It is reasonable to suppose that the AAdS axially symmetric regular solutions discussed in Ref. [20] can be generalized to include a black hole event horizon inside them. The purpose of this paper is to present numerical arguments for the existence of this type of configurations and to analyze the properties of the axially symmetric EYM-SU(2) black hole solutions, in light of the existing results for the asymptotically flat case, discussing the points where the differences are relevant. The numerical methods used here are similar to the methods succesfully employed for $\Lambda < 0$ axially symmetric regular solutions.

The mass of these solutions is computed by using a counterterm method inspired by the AdS/CFT correspondence. Although further research is clearly necessary, at least some of these solutions, emerging as consistent reduction of $d = 11$ supergravity on a seventh dimenensional sphere [27], may have a relevance in AdS/CFT context. In this case the four-dimensional cosmological constant is completely fixed by the gauge coupling constant and exact solutions for configurations preserving some amount of supersymmetry are likely to exist.

The paper is structured as follows: in the next Section we explain the model and derive the basic equations, while in Section 3 we present a detailed computation of the physical quantities of the solutions such as mass, magnetic charge, temperature and entropy noting the relevance of a special class of solutions in $d = 11$ supergravity. In Section 4 solutions of YM equations in a fixed SAdS background are discussed. Some features of the axially symmetric solutions possessing a net YM electric charge in a fixed SAdS black hole background are also presented in this Section. The general properties of the axially symmetric gravitating solutions are presented in Section 5 where we show results obtained by numerical calculations. We give our conclusions and remarks in the final section. The Appendix contains a derivation of an exact solution of the EYM equations with negative cosmological constant with a planar symmetry.

2 GENERAL FRAMEWORK AND EQUATIONS OF MOTION

2.1 Einstein-Yang-Mills action

We will follow in this work most of the conventions and notations used by Kleihaus and Kunz in their papers on asymptotically flat EYM black holes [23], [24]-[26].

The equations for a static, axially symmetric SU(2) gauge field coupled to Einstein gravity with a cosmological term have been presented in Ref. [20]. The starting point is the EYM action

$$I = \int d^4x \sqrt{-g} [\frac{1}{16\pi G}(\mathcal{R} - 2\Lambda) - \frac{1}{2}Tr(F_{\mu\nu}F^{\mu\nu})] - \frac{1}{8\pi G}\int_{\partial\mathcal{M}} d^3x \sqrt{-h}K, \tag{1}$$

where the field strength tensor is

$$F_{\mu\nu} = \partial_\mu A_\nu - \partial_\nu A_\mu + ie[A_\mu, A_\nu] \ , \tag{2}$$

and the gauge field $A_\mu = \frac{1}{2}\tau^a A_\mu^{(a)}$, where e and G are the Yang-Mills (YM) and the gravity coupling constants. The last term in (1) is the Hawking-Gibbons surface term [28], where K is the trace of the extrinsic curvature for the boundary $\partial\mathcal{M}$ and h is the induced metric of the boundary. Of course, this term does not affect the equations of motion but it is relevant for the discussion in Section 3 of the solutions' mass and boundary stress tensor.

Variation of the action (1) with respect to the metric $g^{\mu\nu}$ leads to the Einstein equations

$$R_{\mu\nu} - \frac{1}{2}g_{\mu\nu}R + \Lambda g_{\mu\nu} = 8\pi G T_{\mu\nu}, \tag{3}$$

where the YM stress-energy tensor is

$$T_{\mu\nu} = 2\text{Tr}(F_{\mu\alpha}F_{\nu\beta}g^{\alpha\beta} - \frac{1}{4}g_{\mu\nu}F_{\alpha\beta}F^{\alpha\beta}). \tag{4}$$

Variation with respect to the gauge field A_μ leads to the YM equations

$$\nabla_\mu F^{\mu\nu} + ie[A_\mu, F^{\mu\nu}] = 0. \tag{5}$$

2.2 Static axially symmetric ansatz and gauge condition

As for the globally regular static solutions, we consider a line element on the form

$$ds^2 = g_{\mu\nu}dx^\mu dx^\nu = -fNdt^2 + \frac{m}{f}(\frac{dr^2}{N} + r^2 d\theta^2) + \frac{l}{f}r^2 \sin^2\theta d\varphi^2, \tag{6}$$

where the metric functions f, m and l are only functions of r and θ and we note $N = 1 - \Lambda r^2/3$. Here r is the radial coordinate (we are interested in the region $r_h \le r < \infty$), t is a global time coordinate, (θ, φ) being the usual coordinates on the sphere, with $0 \le \theta \le \pi, 0 \le \varphi < 2\pi$. The metric ansatz (6) generalizes for a nonzero Λ the isotropic axisymmetric line element considered by Kleihaus and Kunz in [23] (a slightly modified version of this metric form has been considered in [8] for asymptotically AdS black holes with abelian Higgs hair). The line element (6) has two Killing vectors: ∂_t coresponding to time translation symmetry and ∂_φ corresponding to rotation symmetry around the $z-$ axis (with $z = r\cos\theta$, $\rho = r\sin\theta$). The event horizon resides at a surface of constant radial coordinate $r = r_h$ and is characterized by the condition $f(r_h) = 0$, while the metric coefficients $g_{rr}, g_{\theta\theta}$ and $g_{\varphi\varphi}$ take nonzero and finite values.

The construction of an axially symmetric YM ansatz has been discussed by many authors starting with the pioneering papers by Manton [29] and Rebbi and Rossi [30]. The most general purely magnetic axially

symmetric YM-SU(2) ansatz contains nine magnetic potentials and can be easily obtained in cylindrical coordinates $x^\mu = (\rho, \varphi, z)$

$$A_\mu = \frac{1}{2} A_\mu^{(\rho)}(\rho, z) \tau_\rho^n + \frac{1}{2} A_\mu^{(\varphi)}(\rho, z) \tau_\varphi^n + \frac{1}{2} A_\mu^{(z)}(\rho, z) \tau_z^n, \tag{7}$$

where the only φ-dependent terms are the $SU(2)$ matrices (composed of the standard (τ_1, τ_2, τ_3) Pauli matrices)

$$\tau_\rho^n = \cos n\varphi \ \tau_1 + \sin n\varphi \ \tau_2, \quad \tau_\varphi^n = -\sin n\varphi \ \tau_1 + \cos n\varphi \ \tau_2, \quad \tau_z^n = \tau_3. \tag{8}$$

Transforming to spherical coordinates, it is convenient to introduce, without any loss of generality, a new SU(2) basis $(\tau_r^n, \tau_\theta^n, \tau_\varphi^n)$, with

$$\tau_r^n = \sin\theta \ \tau_\rho^n + \cos\theta \ \tau_z^n, \quad \tau_\theta^n = \cos\theta \ \tau_\rho^n - \sin\theta \ \tau_z^n. \tag{9}$$

The general expression (7) takes the following form in spherical coordinates

$$A_\mu = \frac{1}{2} A_\mu^{(r)}(r, \theta) \tau_r^n + \frac{1}{2} A_\mu^{(\theta)}(r, \theta) \tau_\theta^n + \frac{1}{2} A_\mu^{(\varphi)}(r, \theta) \tau_\varphi^n, \tag{10}$$

where $A_\mu^{(a)} dx^\mu = A_r^{(a)} dr + A_\theta^{(a)} d\theta + A_\varphi^{(a)} d\varphi$. This ansatz is axially symmetric in the sense that a rotation around the z−axis can be compensated by a gauge rotation $\mathcal{L}_\varphi A = D\Psi$ [31], with Ψ being a Lie-algebra valued gauge function. For the ansatz (10), $\Psi = n \cos\theta \tau_r^n / 2 - n \sin\theta \tau_\theta^n / 2$. Therefore we find $F_{\mu\varphi} = D_\mu W$, where $W = A_\varphi - \Psi$.

Searching for axially symmetric solutions within the most general ansatz is a difficult task, and, to our knowledge there are no analytical or numerical results in this case. We use in this paper a reduced ansatz, employed also in all previous studies on EYM solutions, with five of the gauge potentials taken identically zero

$$A_r^{(r)} = A_r^{(\theta)} = A_\theta^{(r)} = A_\theta^{(\theta)} = A_\varphi^{(\varphi)} = 0.$$

A suitable parametrization of the four nonzero components of $A_\mu^{(a)}$ which factorizes the trivial θ-depencence is

$$A_r^{(r)} = \frac{H_1(r, \theta)}{r}, \ A_\theta^{(r)} = 1 - H_2(r, \theta), \ A_\varphi^{(r)} = -n \sin\theta H_3(r, \theta), \ A_\varphi^{(\theta)} = -n \sin\theta (1 - H_4(r, \theta)), \tag{11}$$

This consistent reduction of the general ansatz satisfies also some additional discrete symmetries [30], [32] (in particular the parity reflection symmetry). The explicit expression of the field strength tensor for this ansatz is given in [25]. To fix the residual abelian gauge invariance we choose the usual gauge condition [23]-[26]

$$r\partial_r H_1 - \partial_\theta H_2 = 0.$$

The ansatz (10) contains an integer n, representing the winding number with respect to the azimutal angle φ. While φ covers the trigonometric circle once, the fields wind n times around. Note that the usual spherically symmetric static ansatz corresponds to $n = 1$, $H_1 = H_3 = 0$, $H_2 = H_4 = w(r)$. Similar to $n = 1$ solutions, we define the node number k by the number of nodes of the gauge fields H_2 and H_4. From (3) and (5) we obtain a set of seven nonlinear elliptical partial differential equations for (f, l, m, H_i) which should be solved numerically. These equations are presented in [20].

Within this ansatz, the energy density of the matter fields $\epsilon = -T_t^t$ is given by

$$-T_t^t = \frac{f^2}{2e^2 r^4 m} \left[\frac{N}{m} (r\partial_r H_2 + \partial_\theta H_1)^2 + \frac{n^2 N}{l} \left((r\partial_r H_3 - H_1 H_4)^2 + (r\partial_r H_4 + H_1(H_3 + \cot\theta))^2 \right) \right. \tag{12}$$

$$\left. + \frac{n^2}{l} \left((\partial_\theta H_3 - 1 + \cot\theta H_3 + H_2 H_4)^2 + (\partial_\theta H_4 + \cot\theta(H_4 - H_2) - H_2 H_3)^2 \right) \right].$$

4

2.3 Boundary conditions

To obtain asymptotically AdS solutions with a regular event horizon and with the proper symmetries, we must impose the appropriate boundary conditions, the boundaries being the horizon and radial infinity, the z-axis and, because of parity reflection symmetry satisfied by the matter fields, the ρ-axis. The boundary conditions at infinity and along the $z-$ and the ρ-axis (i.e for $\theta = 0, \pi/2$) agree with those of the globally regular solutions [20].

Similar to the $\Lambda = 0$ case, we impose the horizon of the black hole to reside at a surface of constant radial coordinate $r = r_h$.

The boundary conditions satisfied by the metric functions are

$$f|_{r=r_h} = m|_{r=r_h} = l|_{r=r_h} = 0, \tag{13}$$

$$f|_{r=\infty} = m|_{r=\infty} = l|_{r=\infty} = 1. \tag{14}$$

We impose also the condition

$$m|_{\theta=0} = l|_{\theta=0}, \tag{15}$$

which is implied by the assumption of regularity on the $z-$axis [33]. The boundary conditions satisfied by the matter functions are very similar to those satisfied in the $\Lambda = 0$ case

$$H_1|_{r=r_h} = 0, \quad \partial_r H_2|_{r=r_h} = \partial_r H_3|_{r=r_h} = \partial_r H_4|_{r=r_h} = 0, \tag{16}$$

at the event horizon and

$$H_2|_{r=\infty} = H_4|_{r=\infty} = \omega_0, \quad H_1|_{r=\infty} = H_3|_{r=\infty} = 0, \tag{17}$$

at infinity, where this time w_0 is a constant (with $w_0 = \pm 1$ for $\Lambda = 0$). The relations (16) come from the condition $F_{r\varphi}|_{r=r_h} = F_{r\theta}|_{r=r_h} = 0$ imposed by the field equations, together with a special gauge choice on the event horizon [26, 34]. For a solution with parity reflection symmetry, the boundary conditions along the axes are

$$\begin{array}{rclcl} H_1|_{\theta=0,\pi/2} & = & H_3|_{\theta=0,\pi/2} & = & 0, \\ \partial_\theta H_2|_{\theta=0,\pi/2} & = & \partial_\theta H_4|_{\theta=0,\pi/2} & = & 0, \end{array} \tag{18}$$

$$\partial_\theta f|_{\theta=0,\pi/2} = \partial_\theta m|_{\theta=0,\pi/2} = \partial_\theta l|_{\theta=0,\pi/2} = 0. \tag{19}$$

Therefore we need to consider the solutions only in the region $0 \leq \theta \leq \pi/2$. Regularity on the $z-$axis requires also

$$H_2|_{\theta=0} = H_4|_{\theta=0}. \tag{20}$$

Dimensionless quantities are obtained by using the following rescaling

$$r \to (\sqrt{4\pi G}/e)r, \quad \Lambda \to (e^2/4\pi G)\Lambda, \quad M \to (eG/\sqrt{4\pi G})M, \tag{21}$$

where M is the mass of the solutions (defined in the next section).

3 PHYSICAL QUANTITIES OF THE SOLUTIONS

3.1 Mass and boundary stress tensor

At spatial infinity, the line element (6) can be written as

$$ds^2 = ds_0^2 + c_{\mu\nu}dx^\mu dx^\nu, \tag{22}$$

where $c_{\mu\nu}$ are deviations from the background AdS metric ds_0^2. Similar to the asymptotically flat case, one expects the value of mass to be encoded in the functions $c_{\mu\nu}$. The construction of the conserved quantities for an asymptotically AdS spacetime was addressed for the first time in the eighties, with various aproaches

(see for instance Ref. [35, 36]). The generalization of Komar's formula in this case is not straightforward and requires the further subtraction of a background configuration in order to render a finite result. The mass of the axially symmetric regular solutions discussed in [20] has been computed in this way, by using the Hamiltonian formalism of Henneaux and Teitelboim [36].

Here we prefer to use a different approach and to follow the general procedure proposed by Balasubramanian and Kraus [37] to compute conserved quantities for a spacetime with a negative cosmological constant. This technique was inspired by AdS/CFT correspondence and consists in adding suitable counterterms I_{ct} to the action. These counterterms are built up with curvature invariants of a boundary $\partial \mathcal{M}$ (which is sent to infinity after the integration) and thus obviously they do not alter the bulk equations of motion.

The following counterterms are sufficient to cancel divergences in four dimensions, for vacuum solutions with a negative cosmological constant

$$I_{\mathrm{ct}} = -\frac{1}{8\pi G} \int_{\partial \mathcal{M}} d^3 x \sqrt{-h} \left[\frac{2}{\tilde{l}} + \frac{\tilde{l}}{2} \mathrm{R} \right] \ . \tag{23}$$

Here R is the Ricci scalar for the boundary metric h. In this section we will define also $\tilde{l}^2 = -3/\Lambda$.

Using these counterterms one can construct a divergence-free stress tensor from the total action $I = I_{\mathrm{bulk}} + I_{\mathrm{surf}} + I_{\mathrm{ct}}$ by defining

$$T_{ab} \quad = \quad \frac{2}{\sqrt{-h}} \frac{\delta I}{\delta h^{ab}} = \frac{1}{8\pi G} (K_{ab} - K h_{ab} - \frac{2}{\tilde{l}} h_{ab} + \tilde{l} E_{ab}), \tag{24}$$

where E_{ab} is the Einstein tensor of the intrinsic metric h_{ab}. The efficiency of this approach has been demonstrated in a broad range of examples, the counterterm subtraction method being developed on its own interest and applications. If there are matter fields on $\mathcal{M}$ additional counterterms may be needed to regulate the action (see e.g. [38]). However, we find that for a SU(2) nonabelian matter content in four dimensions, the prescription (23) removes all divergences (a different situation is found for the five dimensional AAdS nonabelian solutions where the counterterm method fails and logarithmic divergences are presented in the total action and the expression of mass [18]).

In deriving the explicit expression of T_{ab} for our solutions, we make use of the asymptotic behavior of the metric functions

$$f = 1 + \frac{f_1 + f_2 \sin^2 \theta}{r^3} + O(\frac{1}{r^5}), \quad m = 1 + \frac{m_1 + m_2 \sin^2 \theta}{r^3} + O(\frac{1}{r^5}), \quad l = 1 + \frac{l_1 + l_2 \sin^2 \theta}{r^3} + O(\frac{1}{r^5}), \tag{25}$$

where f_1, f_2 are undetermined constants, while

$$l_1 = m_1 = \frac{2f_1}{3}, \quad l_2 = \frac{6f_2}{17}, \quad m_2 = \frac{14f_2}{17}, \tag{26}$$

(note that we find a different power decay as compared with the $\Lambda = 0$ case [25]).

The nonvanishing components of the boundary stress tensor at large r are

$$
\begin{aligned}
T_{\theta\theta} \quad &= \quad -\frac{1}{8\pi G \tilde{l} r} \left(\frac{2f_1}{3} + \frac{6f_2}{17} \sin^2 \theta \right) + O\left(\frac{1}{r^2} \right), \\
T_{\varphi\varphi} \quad &= \quad -\frac{\sin^2 \theta}{8\pi G \tilde{l} r} \left(\frac{2f_1}{3} + \frac{18f_2}{17} \sin^2 \theta \right) + O\left(\frac{1}{r^2} \right), \\
T_{tt} \quad &= \quad -\frac{1}{8\pi G \tilde{l}^3 r} \left(\frac{4f_1}{3} + \frac{24f_2}{17} \sin^2 \theta \right) + O\left(\frac{1}{r^2} \right).
\end{aligned}
\tag{27}
$$

Direct computation shows that this stress tensor is traceless. This result is expected from the AdS/CFT correspondence, since even dimensional bulk theories with $\Lambda < 0$ are dual to odd dimensional CFTs which have a vanishing trace anomaly.

6

We can use this formalism to assign a mass to our EYM solutions by writing the boundary metric in the following form [37]

$$h_{\mu\nu}dx^\mu dx^\nu = -N_\Sigma^2 dt^2 + \sigma_{ab}(dx^a + N_\sigma^a dt)(dx^b + N_\sigma^b dt). \tag{28}$$

If ξ^μ is a Killing vector generating an isometry of the boundary geometry, there should be an associated conserved charge. The conserved charge associated with time translation is the mass of spacetime

$$M = \int_{\partial\Sigma} d^2 x \sqrt{\sigma} N_\Sigma \epsilon \tag{29}$$

(in the absence of an electric part of the YM potential, $N_\sigma^a = 0$ and the solutions carry no angular momentum). Here Σ is a spacelike hypersurface from event horizon to infinity with timelike unit normal n^μ and $\epsilon = n^\mu n^\nu T_{\mu\nu}$ is the proper energy density. By using this relation, we find that the mass of our solutions is given by

$$M = \frac{\Lambda}{3G}\left(\frac{2f_1}{3} + \frac{8f_2}{17}\right). \tag{30}$$

The metric restricted to the boundary h_{ab} diverges due to an infinite conformal factor $r^2/\tilde{l}^2$. The background metric upon which the dual field theory resides is

$$\gamma_{ab} = \lim_{r\to\infty}\frac{\tilde{l}^2}{r^2}h_{ab}.$$

For the asymptotically AdS solutions considered here, the boundary metric is

$$\gamma_{ab}dx^a dx^b = \tilde{l}^2(d\theta^2 + \sin^2\theta d\varphi^2) - dt^2, \tag{31}$$

which is just the line-element of the $(2+1)$ Einstein universe. Corresponding to the boundary metric (31), the stress-energy tensor $<\tau_{ab}>$ for the dual theory can be calculated using the following relation [39]

$$\sqrt{-\gamma}\gamma^{ab} < \tau_{bc} > = \lim_{r\to\infty}\sqrt{-h}h^{ab}T_{bc}. \tag{32}$$

By using this prescription, we find that the stress tensor of the field theory has the curious form

$$< \tau_b^a > = A\,\mathrm{diag}(1,1,-2) + B\,\mathrm{diag}(1,3,-4)\sin^2\theta, \quad \text{with } A = \frac{1}{8\pi\tilde{l}^2}(M + \frac{8f_2}{17}\frac{1}{G\tilde{l}^2}), \ B = -\frac{1}{8\pi G\tilde{l}^4}\frac{6f_2}{17}, \tag{33}$$

where $x^1 = \theta$, $x^2 = \varphi$, $x^3 = t$. Here M, f_2 are continuous variables which encode the bulk parameters. This tensor is covariantly conserved and manifestly traceless. A winding number $n > 1$ of the bulk configurations implies $f_2 \neq 0$ and thus a $\theta-$dependence of the dual theory stress tensor (although the boundary metric is spherically symmetric), which is a unique property of AAdS gravitating nonabelian configurations. This also suggests the dual theory should also contain the integer n.

From the AdS/CFT correspondence, we expect the nonabelian hairy black holes to be described by some thermal states in a dual theory formulated in a $(2+1)$ Einstein Universe background. The spherically and axially symmetric solitons will correspond to zero-temperature states in the same theory. However, for the EYM action (1) we do not know the underlying boundary CFT. In particular, we do not know what the SU(2) field corresponds to in CFT language. The bulk YM fields have nothing to do, of course, with the nonabelian fields of the dual gauge theory. Further work in this direction will be of great interest.

3.2 From $\Lambda = -3$, $d = 4$ EYM to $d = 11$ supergravity

However, the EYM solutions with a negative cosmological constant $\Lambda = -3$ may have some relevance in AdS/CFT context (we'll work in this section with rescaled quantities as defined by (21)). As proven in

[27], for this value of the cosmological constant, an arbitrary solution $(g_{\mu\nu}, A_\mu^{(a)})$ of the four dimensional EYM equations (3), (5) gives a solution of the equations of motion of the $d = 11$ supergravity (note also that the EYM system with $\Lambda > 0$ can also be embedded in $d = 11$ supergravity [40]).

Since this reduction of the eleven dimensional theory has been explained in detail in [27], we present here only the basic results. The Lagrangian of the bosonic sector of $d = 11$ supergravity comprises the eleven-dimensional metric tensor $\hat{g}_{MN}$ and a 4-index antisymmetric tensor field $\hat{F}_{MNPQ}$. Following [27], the eleven dimensional metric ansatz reads (with μ, $\nu \ldots$ denoting indices of the four dimensional space, $M, N \ldots$ indices of the eleventh dimensional solution, while $m, n, \ldots$ are indices on the internal space)

$$d\hat{s}^2 = \hat{g}_{MN}dx^M dx^n = g_{\mu\nu}dx^\mu dx^\nu + g_{mn}(y)(dy^m - K^{(a)m}A_\mu^{(a)}(x)dx^\mu)(dy^n - K^{(a)n}A_\nu^{(a)}(x)dx^\nu), \quad (34)$$

where $g_{\mu\nu}dx^\mu dx^\nu = e^\alpha \otimes e^\beta \eta_{\alpha\beta}$ is the four-dimensional metric (6), $g_{mn}dy^m dy^n = e^p \otimes e^q \delta_{pq}$ is the metric on a round 7-sphere, (e^α, e^p) being the orthonormal bases on these subspaces. $K^{(a)m}$ are three Killing vectors of the seventh dimensional internal space generating the SU(2) Lie algebra.

The antisymmetric tensor field $\hat{F}$ can be read from ($F^{(a)\mu\nu}$ being a solution of the four dimensional YM equations)

$$\hat{F} = \frac{3}{2}\varepsilon_4 - \frac{1}{8}\tilde{G}_{\alpha\beta}^{(a)}M_{cd}^{(a)}\hat{e}^\alpha \wedge \hat{e}^\beta \wedge \hat{e}^c \wedge \hat{e}^d, \quad (35)$$

where $\varepsilon_4 = (4!)^{-1}\varepsilon_{\alpha\beta\gamma\delta}\hat{e}^\alpha \wedge \hat{e}^\beta \wedge \hat{e}^\gamma \wedge \hat{e}^\delta$, $\tilde{G}_{\alpha\beta}^{(a)} = 1/2\varepsilon_{\alpha\beta\mu\nu}F^{(a)\mu\nu}$, while $M_{mn}^{(a)} = -2\nabla_m K_n^{(a)}$.

This embedding suggests the possible existence of BPS configurations with $\Lambda = -3$, satisfying first order differential equations which may lead to exact solutions. An exact solution of the field equations where the round two-sphere (θ, φ) is replaced by a two-dimensional space of vanishing curvature is presented in Appendix.

3.3 Temperature and entropy

The zeroth law of black hole physics states that the surface gravity κ is constant at the horizon of the black hole solutions, where

$$\kappa^2 = -(1/4)g^{tt}g^{ij}(\partial_i g_{tt})(\partial_j g_{tt})\Big|_{r=r_h}. \quad (36)$$

To evaluate κ, we use the following expansions of the metric functions at the horizon

$$
\begin{aligned}
f(r,\theta) &= f_2(\theta)\left(\frac{r-r_h}{r_h}\right)^2 + O\left(\frac{r-r_h}{r_h}\right)^3, \\
m(r,\theta) &= m_2(\theta)\left(\frac{r-r_h}{r_h}\right)^2 + O\left(\frac{r-r_h}{r_h}\right)^3 \\
l(r,\theta) &= l_2(\theta)\left(\frac{r-r_h}{r_h}\right)^2 + O\left(\frac{r-r_h}{r_h}\right)^3.
\end{aligned} \quad (37)
$$

Since from general arguments the temperature T is proportional to the surface gravity κ, $T = \kappa/(2\pi)$, we obtain the relation

$$T = \frac{f_2(\theta)(1 - \Lambda r_h^2/3)}{2\pi r_h \sqrt{m_2(\theta)}}. \quad (38)$$

Similar to the $\Lambda = 0$ case, we can show, with help of the $(r\ \theta)$ Einstein equation which implies

$$f_2 m_{2,\theta} = 2m_2 f_{2,\theta}, \quad (39)$$

that the temperature T, as given in (38), is indeed constant.

For the line element (6), the area A of the event horizon is given by

$$A = 2\pi \int_0^\pi d\theta \sin\theta \frac{\sqrt{l_2(\theta)m_2(\theta)}}{f_2(\theta)}r_h^2. \quad (40)$$

8

According to the usual thermodynamic arguments, the entropy S is proportional to the area A [49]

$$S = \frac{A}{4G}, \tag{41}$$

leading to the product

$$TS = \frac{r_h(1 - \Lambda r_h^2/3)}{4G} \int_0^\pi d\theta \sin\theta \sqrt{l_2(\theta)}. \tag{42}$$

Unfortunatelly, for $\Lambda < 0$ we could not derive a simple Smarr-type relation, similar to that valid for asymptotically flat hairy black holes [23], which relates asymptotic quantities to quantities defined on the event horizon (this relation can also be used to test the accuracy of the numerical results). When integrating the Killing identity

$$\nabla^a \nabla_b K_a = R_{bc} K^c, \tag{43}$$

for the Killing field $K^a = \delta_t^a$ over a spacelike hypersurface Σ, we find the expression

$$-\frac{1}{2} \int_0^\pi d\theta \sin\theta \frac{r^2\sqrt{l}}{f}\left(N\partial_r f - \frac{2\Lambda r}{3}f\right)\Big|_{r_h}^\infty = \Lambda \int_{rh}^\infty dr \int_0^\pi d\theta \sin\theta \frac{r^2 m\sqrt{l}}{f} + 8\pi G \int_{rh}^\infty dr \int_0^\pi d\theta \sin\theta \frac{r^2 m\sqrt{l}}{f} T_t^t, \tag{44}$$

(here we use $R = 4\Lambda$ and $T_\mu^\mu = 0$). To make sense on this expression we must regularize it, by extracting a background contribution ($g_{\mu\nu}^0$). However, this gives useful results for very simple configurations only (with $\sqrt{-g} = \sqrt{-g^0}$). This background subtraction is of no practical use for numerical solutions like ours.

3.4 A computation of the Euclidean action

The expression (41) for the entropy can be derived in a more rigorous way by using Euclidean quantum gravity arguments. Here we start by constructing the path integral [28]

$$Z = \int D[g]D[\Psi]e^{-iI[g,\Psi]} \tag{45}$$

by integrating over all metrics and matter fields between some given initial and final hypersurfaces, Ψ corresponding here to the SU(2) potentials. By analytically continuing the time coordinate $t \to i\tau$, the path integral formally converges, and in the leading order one obtains

$$Z \simeq e^{-I_{cl}} \tag{46}$$

where I_{cl} is the classical action evaluated on the equations of motion of the gravity/matter system. We note that the considered Lorentzian solutions of the EYM equations extremize also the Euclidean action, $t \to i\tau$ having no effects at the level of the equations of motion [3]. The value of β is found here by demanding regularity of the Euclideanized manifold as $r \to r_h$, which together with the expansion (37) and the condition (39) gives $\beta = 1/T$. The physical interpretation of this formalism is that the class of regular stationary metrics forms an ensemble of thermodynamic systems at equilibrium temperature T [41]. Z has the interpretation of partition function and we can define the free energy of the system $F = -\beta^{-1}\log Z$. Therefore

$$\log Z = -\beta F = S - \beta M, \tag{47}$$

or

$$S = \beta M - I_{cl}, \tag{48}$$

straightforwardly follows.

---

[3]Note that this analytical continuation becomes problematic for nonabelian solutions with an electric potential.

To compute I_{cl}, we make use of the Einstein equations, replacing the $R - 2\Lambda$ volume term with $2R_t^t - 16\pi G T_t^t$. For our purely magnetic ansatz, the term T_t^t exactly cancels the matter field lagrangean in the bulk action $L_m = -1/2 Tr(F_{\mu\nu}F^{\mu\nu})$. The divergent contribution given by the surface integral term at infinity in R_t^t is also canceled by $I_{\text{surface}} + I_{ct}$ and we arrive at the simple finite expression

$$I_{cl} = \beta \left(\frac{\Lambda}{3G} \left(\frac{2f_1}{3} + \frac{8f_2}{17} \right) - \frac{r_h}{4G} \left(1 - \frac{\Lambda r_h^2}{3} \right) \int_0^\pi d\theta \sin\theta \sqrt{l_2(\theta)} \right) \tag{49}$$

Replacing now in (48) (where M is the mass-energy computed in Section 3.1), we find

$$S = \frac{\pi}{2G} \int_0^\pi d\theta \sin\theta \frac{\sqrt{l_2(\theta)m_2(\theta)}}{f_2(\theta)} r_h^2, \tag{50}$$

which is one quarter of the event horizon area, as expected.

3.5   Nonabelian charges

Solutions of the field equations are also classified by the nonabelian electric and magnetic charges Q_E and Q_M. For purely magnetic configurations, the usual definition used by various authors (and employed also in this paper) is

$$Q_M = \frac{e}{4\pi} \int dS_k \sqrt{-g} Tr\{\tilde{F}^{k0}\tau_r\}, \tag{51}$$

where $\tilde{F}^{\mu\nu}$ is the dual field strength tensor. For the boundary conditions at infinity (17), we find $Q_M = n(1-\omega_0^2)$. However, the integral (51) does not intrinsically characterize a field configuration, as it is gauge dependent. A gauge invariant definition for the nonabelian charges has been proposed in [42] and used in [26] for asymptotically flat nonabelian solutions

$$Q_E = \frac{e}{4\pi} \oint d\theta d\varphi |\tilde{F}_{\theta\varphi}|, \quad Q_M = \frac{e}{4\pi} \oint d\theta d\varphi |F_{\theta\varphi}|, \tag{52}$$

where the vertical bars denote the Lie-algebra norm and the integrals are evaluated as $r \to \infty$. One can verify that this definition yields the absolute value of the magnetic charge as defined in (51).

4   YANG-MILLS FIELDS IN FIXED BLACK HOLE BACK-GROUND

For asymptotically AdS geometries, it has been proven useful in a number of cases to consider first the matter system in a fixed background, as a first step toward the study of the gravitating configurations. These solutions preserve the basic features of the gravitating counterparts and can be obtained much more easily. This situation resembles the well-known case of (asymptotically-) flat monopoles and dyons, where the inclusion of gravity does not change the essential picture.

In this section we present numerical arguments for the existence of nontrivial monopoles and dyons solutions of pure YM equations in a four dimensional SAdS black hole background, gravity being regarded as a fixed external field. Although being very simple, nevertheless this model appears to contain all the essential features of the gravitating black hole solutions.

The background metric is given by

$$\begin{aligned} ds^2 &= \frac{dr^2}{F} + r^2(d\theta^2 + \sin^2\theta d\varphi^2) - F dt^2, \\ F &= 1 - \frac{2\tilde{M}}{r} - \frac{\Lambda r^2}{3}, \end{aligned} \tag{53}$$

where $\tilde{M}$ is the black hole mass, and the black hole horizon r_h is located at the largest root of the equation $r_h - 2\tilde{M} - \Lambda r_h^3/3 = 0$. Note that this line element is not on the form (6); unfortunately, the SAdS metric does not present a simple form in "isotropic" coordinates and we should make use of the usual Schwarzschild coordinates.

4.1 Monopole solutions

4.1.1 Spherically symmetric configurations

We start by briefly discussing the solutions obtained for $n = 1$ within the magnetic ansatz (11). In this case $H_1 = H_3 = 0$, $H_2 = H_4 = \omega(r)$ and the YM equations have the simple form

$$\omega'' = \frac{1}{F}\left[\frac{\omega(\omega^2-1)}{r^2} - (\frac{2\tilde{M}}{r^2} - \frac{2\Lambda r}{3})\omega'\right], \tag{54}$$

where the prime denotes derivative with respect to r. This problem possesses two nontrivial limits, with known exact solutions, noticed for the first time in [43]. The first one is found for $M \to 0$

$$\omega = \frac{1}{\sqrt{1 - \Lambda/3r^2}}, \tag{55}$$

describing a monopole in AdS spacetime with unit magnetic charge. Apart from this exact solution, a continuous family of $k = 0$ finite energy configurations is found [20, 44]. Even more remarkable, the second one valid as $\Lambda \to 0$ describes a nonabelian hair for a Schwarzschild black hole

$$\omega = \frac{c-r}{r+3(c-1)}, \tag{56}$$

where $c = M(3 + \sqrt{3})$. In this case, we find an infinite sequence of excited solutions, indexed by the node number k (the solution (56) corresponds to $k = 1$), with similar properties to the well known gravitating counterparts [45]).

In the $\Lambda < 0$ case, the numerical results show the existence of a one-parameter family of solutions regular at $r = r_h$ with the following behavior as $r \to r_h$

$$\omega(r) = \omega_h + \frac{\omega_h(\omega_h^2-1)}{r_h(1-\Lambda r_h^2)}(r-r_h) + O(r-r_h)^2, \tag{57}$$

and the asymptotic expansion at large r

$$\omega = \omega_0 + \frac{w_1}{r} + O(\frac{1}{r^2}), \tag{58}$$

where ω_0, ω_1 are constants to be determined by numerical calculations and there are no restrictions on the value of ω_0. Since the field equations are invariant under the transformation $\omega \to -\omega$, only values of $\omega_h > 0$ are considered. The boundary condition (58) permits a non-vanishing magnetic charge $Q_M = 1 - \omega_0^2$.

The overall picture we find for the general case is rather similar to the one described in [11] where gravity is taken into account. By varying the parameter ω_h, a continuum of monopole solutions is obtained. The same general behavior is noticed for the gauge function ω, with very similar branch structure. As expected, the properties of the solutions depends esentially on the values of Λ, r_h. For $|\Lambda|$ sufficiently large, there exist finite energy solutions for which the gauge function has no nodes. Values of $\omega_h > 1$ are always allowed, leading to nodeless solutions. For a fixed value of Λ, we obtain finite energy solutions for a finite number of intervals in parameter space. We noticed always the existence of at least two such interval around the trivial solutions $\omega_h = 1,\ 0$. For large enough values of $|\Lambda|$, the ω function remain close to its initial value on the event horizon, and we find only one branch of solutions. For small enough $|\Lambda|$, we have found solutions where ω crosses the r axis and a large number of branches. The arguments presented in [11] for the (linear) stability of the nodeless $n = 1$ monopole solutions apply directly to the nongravitating case.

11

4.1.2 Axially symmetric configurations

The next step is to consider the $n > 1$ axially symmetric generalizations of these configurations. Subject to the boundary conditions (13)-(19), we solve numerically for a fixed SAdS background the set of four YM equations implied by (5).

The algorithm we have used for all axially symmetric solutions presented in this paper is only a slightly modified version of the approach employed by Kleihaus and Kunz in their studies of asymptotically flat nonabelian configurations. The field equations are first discretized on a (r, θ) grid with $N_r \times N_\theta$ points. The angular coordinate θ runs from 0 to $\pi/2$ and the radial coordinate goes from r_h to some large enough value r_{max} (this value is not fixed apriori, depending on the parameters r_h, Λ; typically $r_{max} \simeq 3 \times 10^3 \div 6 \times 10^3 r_h$). We tested for a number of solutions that the relevant quantities are insensitive to the cut off value r_{max}. The grid spacing in the $r-$direction is non-uniform, while the values of the grid points in the angular direction are given by $\theta_k = (k-1)\pi/(2(N_\theta - 1))$. Essentially, our numerical problems come from the region near the event horizon, where a carefull grid choice is necessary.

In this scheme, a new radial variable is introduced which maps the semi infinite region $[r_h, \infty)$ to the closed region $[0, 1]$. Our choice for this transformation was $x = (r - r_h)/(r + c)$, where c is a properly chosen constant in order to minimize the numerical errors. A $c \neq 0$ proven to be useful for higher mass solutions (however in most of the computations c takes a value smaller than 20). Typical grids have sizes 150×30, covering the integration region $0 \leq x \leq 1$ and $0 \leq \theta \leq \pi/2$. The resulting system is solved iteratively until convergence is achieved. All numerical calculations for axially symmetric configurations are performed by using the program FIDISOL (written in Fortran), based on the iterative Newton-Raphson method. Details of the FIDISOL code are presented in [46]. This code requests the system of nonlinear partial differential equations to be written in the form $F(r, \theta, u, u_r, u_\theta, u_{r\theta}, u_{rr}, u_{\theta\theta}) = 0$, (where u denotes the unknown functions) subject to a set of boundary conditions on a rectangular domain. The user must deliver to FIDISOL the equations, the boundary conditions, and the Jacobian matrices for the equations and the boundary conditions. Starting with a guess solution, small corrections are computed until a desired accuracy is reached. FIDISOL automatically provides also an error estimate for each unknown function, which is the maximum of the discretization error divided by the maximum of the function.

The output of the code was analysed and visualised mainly with MATHEMATICA.

To obtain axially symmetric solutions, we start with the $n = 1$ solution as initial guess and increase the value of n slowly. The iterations converge, and repeating the procedure one obtains in this way solutions for arbitrary n. The physical values of n are integers. For some of the configurations, we use these configurations as a starting guess on a finer grid. For magnetic monopoles solutions in a fixed SAdS background, the typical numerical error for the functions is estimated to be lower than 10^{-3}.

The energy density of these nongravitating solutions is given by the tt-component of the energy momentum tensor T^ν_μ; integration over all space yields their total mass-energy

$$M = \int \left\{ \frac{1}{4} F^a_{ij} F^{aij} \right\} \sqrt{-g} d^3x = \pi \int_{r_h}^\infty \int_0^{\pi/2} dr d\theta \ r^2 \sin\theta F^a_{ij} F^{aij}. \tag{59}$$

We have obtained higher winding number generalizations for every spherically symmetric configuration. Also, the branch structure noticed for $n = 1$ is retained for higher winding number solutions. These solutions have very similar properties with the corresponding EYM counterparts and the general picture we present here applies also in the Section 5.

We have studied a large number of configurations with $n = 2, 3, 4$ and node number $k = 0, 1, 2$ in SAdS backgrounds with $r_h = 1$ and various Λ between 10^{-3} and 10^2. It is not easy to extract some general characteristic properties of the solutions, valid for every choice of the parameters $(\Lambda, \omega_0, n, k)$. However, we have found that the functions H_1 and H_3 present always a considerable angle-dependence. With increasing ω_0, the maximal value of the H_1 and H_3 increase. The functions H_2 and H_4 present a small θ dependence, although the angular dependence generally increases with Q_M. The qualitative behavior of the gauge functions does not change by changing the value of Λ (the picture presented in Figure 10 for gravitating gauge functions applies in this case, too).

As a typical example, in Figure 1 the gauge functions H_i and the energy density ϵ are shown for three different solutions with node number $k = 0, 1$ as a function of the radial coordinate r at angles $\theta = 0$, $\pi/4$, $\pi/2$. Here the winding number is $n = 3$ and $\Lambda = -0.01$, $r_h = 1$; also the energy density is given in units $4\pi/e^2$. We notice that the gauge field function H_1 remains nodeless and for every solution with $w_0 > 1$ it takes only negative values (H_1 and H_3 are zero on the axes in Fig. 1a and 1c). The behavior of the energy density strongly depends on the value of ω_0. For example, as seen in Figure 1e, for the $k = 1$ solution, the global maximum of the energy density resides on the ρ axis, for a $r > r_h$. Surfaces of constant energy density for nongravitating solutions have a similar form to those presented in Section 5 in the presence of gravity and we will not present them here.

The monopole spectrum is presented in Figure 2 for a SAdS black hole with $\Lambda = -3$, $r_h = 1$. In this case, the existence of one branch of solutions was noticed, and the monopole mass strongly increases with the magnetic charge.

4.2 Nongravitating dyon solutions

Following [20], we present here numerical arguments for the existence of finite energy nongravitating YM dyon solutions in a fixed SAdS background. The existence of dyon solutions without a Higgs field is a new feature for AdS spacetime [11]. This is a consequence of the different asymptotic behavior of the AdS geometries as compared to the asymptotically flat case. If $\Lambda \geq 0$ the electric part of the gauge fields is forbidden for static configurations [11, 47]. In order for the boundary conditions at infinity to permit the electric fields and maintain a finite ADM mass we have to add scalar fields to the theory.

The YM axially symmetric ansatz (11) can be generalized to include an electric part (see $e.g.$ [26, 48])

$$A_t = H_5(r,\theta)\frac{\tau_r^n}{2e} + H_6(r,\theta)\frac{\tau_\theta^n}{2e}. \tag{60}$$

For the time translation symmetry, we choose a natural gauge such that $\partial A/\partial t = 0$.

For $A_t \neq 0$, the total energy (59) should be supplemented by an electric contribution

$$
\begin{aligned}
E_e &= \frac{1}{4}\int F_{it}^a F^{ait}\sqrt{-g}d^3x \\
&= \pi\int_{r_h}^{\infty}\int_0^{\pi/2} drd\theta \sin\theta\Big((r\partial_r H_5 + \frac{H_1 H_6}{r})^2 + (r\partial_r H_6 - \frac{H_1 H_5}{r})^2 \\
&\quad + \frac{1}{r^2 F}\left((\partial_\theta H_5 - H_2 H_6)^2 + (\partial_\theta H_6 + H_2 H_5)^2 + n^2(H_6(H_3 + \cot\theta) + H_4 H_5)^2\right)\Big).
\end{aligned}
\tag{61}
$$

We can use the existence of the Killing vector $\partial/\partial t$ which implies $F_{it} = D_i A_t$, and the YM equations (5), to express the "electric mass" (61) as a difference of two surface integrals [49]

$$-E_e = Tr\left(\int\{D_i(A_t F^{it}\sqrt{-g}) - A_t D_i(F^{it}\sqrt{-g})d^3x\}\right) = \oint_\infty Tr\{A_t F^{\mu t}\}dS_\mu - \oint_{r_h} Tr\{A_t F^{\mu t}\}dS_\mu. \tag{62}$$

From the conditions of local finiteness of the energy density, we find that the electric potentials necessarily vanish on the event horizon of a static black hole (for a rotating background, the situation may be different). Thus, the electric mass retains only the asymptotic contribution and, similar to the regular case, a vanishing magnitude of the electric potentials at infinity $|A_t|$ implies a purely magnetic solution.

Since these axially symmetric solutions have a nonzero electric potential, we may expect them to possess a nonvanishing angular momentum. The total angular momentum of a nongravitating solution is given by

$$J = \int T_\varphi^t\sqrt{-g}d^3x = \int 2Tr\{F_{r\varphi}F^{rt} + F_{\theta\varphi}F^{\theta t}\}\sqrt{-g}d^3x, \tag{63}$$

and can be expressed again as a difference of two surface integrals [50]

$$J = \oint_\infty 2Tr\{WF^{\mu t}\}dS_\mu - \oint_{r_h} 2Tr\{WF^{\mu t}\}dS_\mu. \tag{64}$$

The relations (61)-(64) provide also an useful tests to verify the accuracy of the numerical calculations. The electric charge of the dyon solutions is evaluated by using the definition (52).

4.2.1 Static dyon solutions

A possible set of boundary conditions for the electric potentials H_5, H_6 is

$$H_5|_{r=r_h} = H_6|_{r=r_h} = 0, \quad H_5|_{r=\infty} = u_0, \quad H_6|_{r=\infty} = 0, \tag{65}$$

and

$$\partial_\theta H_5|_{\theta=0,\pi/2} = H_6|_{\theta=0,\pi/2} = 0 \tag{66}$$

for a solution with parity reflection symmetry. The magnetic potentials satisfy the same set of boundary conditions valid in purely magnetic case.

These solutions can be considered the counterparts of the regular YM dyons in a fixed AdS geometry discussed in [20], since they satisfy the same boundary conditions at infinity and on the axes. The presence of a SAdS black hole will affect the properties of these solutions in the event horizon region only. We remark that, although locally $T_\varphi^t \neq 0$, the configurations with the symmetries implying the above boundary conditions along the axes have always $J = 0$. We use the fact that, as $\theta \to \pi - \theta$ we have $H_1 \to -H_1$, $H_2 \to H_2$, $H_3 \to -H_3$, $H_4 \to H_4$, $H_5 \to H_5$, $H_6 \to -H_6$ which implies the vanishing of the integral (63).

Spherically symmetric dyon solutions (discussed in [11] for the gravitating case) are found by taking $n = 1$, $H_5 = u(r)$, $H_2 = H_4 = \omega(r)$ and $H_1 = H_3 = H_6 = 0$. The behavior of the electric potential in a fixed SAdS geometry is

$$u(r) = u_h(r - r_h) + O(r^3), \tag{67}$$

at the event horizon and

$$u = u_0 + \frac{u_1}{r} + O(\frac{1}{r^2}) \tag{68}$$

at large r, where u_h, u_0, u_1 are constants. The expansion (57),(58) for the magnetic gauge function $\omega(r)$ is still valid. These boundary conditions permit non-vanishing charges Q_M and Q_E.

As expected, the general properties of these solutions are rather similar to the gravitating counterparts. There are two adjustable shooting parameters defined on the event horizon (u_h, ω_h). At the horizon, u starts at zero and monotonically increases asymptotically to a finite value. Solutions are found for a continuous set of parameters u_h and ω_h; for some limiting values of these parameters, solutions blow up. Given (u_h, ω_h), the general behavior of the gauge functions w, u is similar to the gravitating case; there are also solutions with $Q_M = 0$ but $Q_E \neq 0$. Similar to the soliton solutions discussed in [11], purely magnetic solutions are obtained by setting $u_h = 0$.

When studying dyon solutions we notice the existence always of higher node $(k > 1)$ configurations, for suitable values of (u_h, ω_h). Also, there are solutions where ω does not cross the r axis. For a fixed value of ω_h, the number of nodes is determined by the value of the parameter u_1. Typical spherically symmetric solutions are displayed in Fig. 3.

The same numerical method described above is used to obtain higher winding number static dyon solutions in a fixed SAdS black hole background (the typical relative error is estimated to be of the order of 10^{-3}). The spherically symmetric $n = 1$ solution gives the input data in the numerical iteration and it fixes the values ω_0, u_0 in the boundary conditions at infinity. Axially symmetric $n > 1$ generalizations seem to exist for every spherically symmetric configuration. Here the inclusion of the electric potential does not seem to change qualitatively the general picture found in the purely magnetic case. As expected, for a given value of the magnetic charge, the total mass of the solutions increases with the electric charge. The shape of the energy density for the monopole solutions is retained for the $n > 1$ dyon solutions.

As typical axially symmetrical static dyon configurations, we show in Figure 4 the radial dependence of the gauge functions H_i and the energy density ϵ (in units $4\pi/e^2$) for three solutions with the same magnetic charge and magnitude of the electric potential at infinity and $n = 1$, 2, 3. The results are given for three different angles. The value of the cosmological constant is $\Lambda = -3$ while the event horizon radius of the SAdS black hole is $r_h = 1$. These solution have been obtained starting from a spherically symmetric configurations with the shooting parameters $\omega_h = 0.9$ and $u_h = 0.03$. As seen in Fig. 4a-f, the gauge functions H_2, H_4, H_5 do not exhibit a strong angular dependence, while the functions H_1, H_3 and H_6 remain nodeless for $\omega_0 > 0$. The angular dependence of the matter functions increases with n and the location of the biggest angular spliting slightly moves further outward with n. The maximal values of the functions H_1, H_3 and H_6 increase also with n, depending on the value of ω_0. Similar results have been obtained for other values of Λ.

4.2.2 Rotating dyon solutions

However, the boundary conditions for the electric potentials H_5 and H_6 (65)-(66) do not exhaust all possibilities even for $n = 1$. Inspired by [19], we have searched for solutions with electric potentials satisfying a different set of boundary conditions (the magnetic potentials satisfiying the same boundary conditions as in the purely magnetic case)

$$H_5|_{r=r_h} = H_6|_{r=r_h} = 0, \quad H_5|_{r=\infty} = V\cos\theta, \quad H_6|_{r=\infty} = V\sin\theta, \tag{69}$$
$$\partial_\theta H_5|_{\theta=0} = H_6|_{\theta=0} = 0, \quad H_5|_{\theta=\pi/2} = \partial_\theta H_6|_{\theta=\pi/2} = 0,$$

where V is a constant corresponding to the magnitude of the electric potential at infinity. The value of the electric charge can be obtained from the asymptotics of the electric potentials, since as $r \to \infty$, $H_5 \sim \cos\theta(V + (c_1\sin^2\theta + c_2)/r)$, $H_6 \sim \sin\theta(V + (c_3\sin^2\theta + c_4)/r)$. We remark that, similar to the regular case, dyon solutions with these symmetries possess a nonzero angular momentum (since the integral (63) is nonvanishing in this case).

As initial guess in the iteration procedure, we use the $n = 1$ static YM solution in fixed SAdS background discussed above and slowly increased the value of V. The typical relative error for the gauge functions is estimated to be on the order of 10^{-3}, while the relations (62) and (64) are satisfied with a very good accuracy. All the solutions we present here have winding number $n = 1$ and have been obtained for a SAdS black hole with $\Lambda = -3$, $r_h = 1$. However, a similar general behavior has been found for some other negative values of Λ. Several solutions with $n = 2$ have been also studied, possessing very similar properties.

The situation here presents a number of similarities to rotating YM dyons in an AdS background [19]. For a given SAdS background, we found nontrivial rotating solutions for every spherically symmetric configuration we have considered. The solutions depend on two continous parameters: the values ω_0 of the magnetic potentials H_2, H_4 at infinity and the magnitude of the electric potential at infinity V. A nonvanishing V leads to rotating configurations, with nontrivial functions H_1, H_3, H_5, H_6 and nonzero Q_E. As we increase V from zero while keeping ω_0 fixed, a branch of solutions forms. This branch extends up to a maximal value of V, which depends on ω_0. Along this branch, the total energy, electric charge, electric part of energy and the absolute value of the angular momentum increase continuously with V. This can be seen in Figure 5, where we present the properties of a typical branch of solutions in a SAdS background, for a fixed value of ω_0. In this picture, the total energy E and the angular momentum J (in units $4\pi/e^2$) as well as the electric charge Q_E and the ratio E_e/E are shown as a function of the parameter V.

Depending on V, the energy of a rotating dyon can be several orders of magnitude greater than the energy of the corresponding monopole solution. We find that both E_e/E and J/E^2 tend to constant values as V is increased. At the same time, the numerical errors start to increase, we obtain large values for both Q_E and E, and for some V_{max} the numerical iterations fail to converge. In this limit, the total energy and the electric charge diverge, while the magnetic charge takes a finite value. It is difficult to find an accurate value for V_{max}, especially for large values of ω_0. Alternatively, we may keep fixed the magnitude of the electric potential at infinity and vary the parameter ω_0.

15

There are also solutions where $Q_M = 0$ and $Q_E \neq 0$. A vanishing Q_E implies a nonrotating, purely magnetic configuration. However, we find dyon solutions with vanishing total angular momentum ($J = 0$ for some ω_0, V) which are not static (locally $T_\varphi^t \neq 0$). For the considered configurations, we have found that most of the angular momentum in (64) comes from the surface integral at infinity contribution, the event horizon integral taking small values.

As a typical axially symmetrical configuration, we show in Figure 6 three-dimensional plots of the gauge functions H_i, the magnitude of the electric potential $|A_t| = (H_5^2 + H_6^2)^{1/2}$, the local angular momentum T_φ^t and the energy density ϵ for a solution with $n = 1$, total energy $E = 6.72$ (in units $4\pi/e^2$), nonabelian charges $Q_M = -3.622$ and $Q_E = 6.833$ as a function of the coordinates ρ and z. We can see that both local energy and angular momentum are localized in a small region around the event horizon without being possible to distinguish any individual component. For the gauge function, the relevant oscillating region extends at least one order of magnitude beyond the event horizon.

For some of the configurations we have considered, the surfaces of constant energy density reveal a curious shape, which is different from the other static solutions considered in this paper or other cases exhibited in the literature (see Figure 6g-i).

In the presence of gravity, the field equations for a rotating dyon configuration are considerably more complicated, the metric ansatz (6) being supplemented with at least one extradiagonal term. However, we expect the gravitating counterparts of these solutions to retain the basic features discussed here.

5   AXIALLY SYMMETRIC SOLUTIONS IN THE PRESENCE OF GRAVITY

Now we come to the main subject of this paper, by including the backreaction of the YM fields on the black hole geometry. In this case, the equations of motion are considerably more complicated than in the pure YM case. This is a difficult numerical problem even for asymptotically flat geometries, where no exact solution is known yet.

5.1   Spherically symmetric EYM solutions

The spherically symmetric EYM black hole solutions presented in [10, 11], have been obtained for a Schwarzschild-like line element

$$ds^2 = -\frac{H(\tilde{r})}{p(\tilde{r})^2}dt^2 + \frac{1}{H(\tilde{r})}d\tilde{r}^2 + \tilde{r}^2 \left(d\theta^2 + \sin^2\theta d\varphi^2\right), \tag{70}$$

where

$$H(\tilde{r}) = 1 - \frac{2\tilde{m}(\tilde{r})}{\tilde{r}} - \frac{\Lambda}{3}\tilde{r}^2.$$

The spherically symmetric horizon resides at radial coordinate $\tilde{r}_h$, solution of the equation $\tilde{r}_h - 2m(\tilde{r}_h) - \Lambda\tilde{r}_h^3/3 = 0$. Since we need the spherically symmetric $n = 1$ solution as the starting point for the calculation of axially symmetric configurations, it is useful to reobtain these solutions by using a different set of coordinates required by the metric ansatz (6).

By imposing $l = m$ and the metric functions f and m to be functions only of the coordinate r, the axially symmetric ansatz (6) reduces to the spherically symmetric form

$$ds^2 = -f(1 - \frac{\Lambda}{3}r^2)dt^2 + \frac{m}{f}\Big(\frac{dr^2}{1 - \frac{\Lambda}{3}r^2} + r^2\left(d\theta^2 + \sin^2\theta d\varphi^2\right)\Big). \tag{71}$$

Of course, for the same configuration, the values of the event horizon radius will differ for these different metric parametrizations (70), (71). Comparison of the metric in Schwarzschild coordinates (70) with the

"isotropic" metric (71) yields

$$\frac{f(r)}{m(r)} = \frac{r^2}{\tilde{r}^2}, \quad \frac{dr}{r\sqrt{1 - \frac{\Lambda}{3}r^2}} = \frac{1}{\sqrt{H(\tilde{r})}} \frac{d\tilde{r}}{\tilde{r}}, \quad f(1 - \frac{\Lambda}{3}r^2) = \frac{H(\tilde{r})}{p(\tilde{r})^2}. \tag{72}$$

Since the mass function $\tilde{m}(\tilde{r})$ is only known numerically, we have to numerically integrate the above relations to obtain the coordinate function $r(\tilde{r})$ and the metric functions $m(r)$, $f(r)$. This is a direct generalization of the method used in [23] for $\Lambda = 0$ EYM solutions and employed also in [20] for regular EYM regular with negative cosmological constant.

However, we have found more convenient to solve directly the $n = 1$ EYM equations by using the line element (71). The field equations read for this parametrization

$$\omega'' - \omega' \left(\frac{m'}{2m} - \frac{f'}{f} + \frac{2\Lambda}{3} \frac{r}{N} \right) - \frac{\omega(\omega^2 - 1)}{r^2 N} = 0,$$

$$f'' - \frac{f'^2}{f} + \frac{f'm'}{2m} + \frac{2f'}{r} - \frac{4f^2}{mr^2} \left(\omega'^2 + \frac{1}{2N} \frac{(\omega^2 - 1)^2}{r^2} \right) - \frac{\Lambda}{N} \left(2f - 2m + \frac{2r}{3}(f' + \frac{m'f}{2m}) \right) = 0, \tag{73}$$

$$m'' - \frac{m'^2}{2m} + \frac{3m'}{r} - \frac{4\omega'^2 f}{r^2} - \frac{\Lambda}{N} \left(rm' + 4m - \frac{4m^2}{f} \right) = 0,$$

and are solved with a set of boundary conditions on the event horizon

$$m = m_2(r - r_h)^2 + O(r - r_h)^3, \quad f = f_2(r - r_h)^2 + O(r - r_h)^3, \quad \omega = \omega_0 + O(r - r_h)^2. \tag{74}$$

Asymptotically we find

$$m = 1 + \frac{m_1}{r^3} + O(\frac{1}{r^5}), \quad f = 1 + \frac{f_1}{r^3} + O(\frac{1}{r^5}), \quad \omega = \omega_0 + \frac{\omega_1}{r} + O(\frac{1}{r^2}). \tag{75}$$

Using these boundary conditions, the equations (73) were integrated for $r_h = 1$ and various values of Λ. Again, only values of $\omega_h > 0$ have been considered. The value $\omega_h = 0$ corresponds to a Reissner-Nordström-AdS solutions, while $\omega_h = 1$ is the vacuum SAdS solution (although these solutions do not have a simple form in this coordinate system).

As expected, the solutions obtained for the metric ansatz (71) present similar properties to those found for the Schwarzschild-like line-element (70). Also, all the basic features of the spherically symmetric nongravitating solutions discussed in Section 4.1. survive in the presence of gravity.

5.2 Properties of the axially symmetric EYM solutions

To find axially symmetric solutions of the purely magnetic EYM equations, we have used the same numerical algorithm as for the YM solutions in a fixed SAdS background presented above. We have started always with a $n = 1$ EYM solution as initial guess and increase the value of n slowly (for a fixed ω_0), until approaching the integer physical values. For every n, corrections are calculated successively, until the numerical solutions satisfies a given tolerance. The typical numerical error for the gravitating solutions is of the order of 10^{-3}, except for some $n = 3$ or $k = 2$ solutions and most of those with $n = 4$, where we found an error on the order of 10^{-2}. This error depends on the magnetic charge and mass of the solutions. Axially symmetric generalizations of the $n = 1$ solutions with a large ratio $M(\omega_0)/M(\omega_0 = 1)$ are difficult to obtain, with large numerical errors. Also, for some of the higher node solutions the convergence is slowed down and the errors are not small enough for the results to be reliable. A set of $\Lambda = 0$ test runs was carried out, primarily designed to evaluate the code's ability to reproduce the Kleihaus-Kunz results. In this case, we have obtained a very good agreement with the results of [23].

The axially symmetric solutions depend on three continuous parameters (r_h, Λ, ω_0) as well as two integers: the winding number $n > 1$ and the node number k. We have considered solutions with $r_h = 1$, several negative values of Λ, the node number $n = 2, 3, 4$ and $k \leq 2$. Special care has been paid to

the properties of the nodeless solutions because these configurations are likely to be stable against linear perturbations.

Once we have a solution, the horizon variables such as T_H, A are calculated in a straightforward way from (38), (40). The mass of the solution is computed by using the relation (30), extracting the values of the coefficients f_1, f_2 from the asymptotics of the metric functions (we used also the asymptotic relation (26) to test the accuracy of our results).

The behavior of the solutions is in many ways similar to that of the axially symmetric solitons discussed in [20]. Again, starting from a spherically symmetric configuration we obtain higher winding number generalizations with many similar properties. Axially symmetric generalizations seem to exist for every spherically symmetric black hole solution. For a fixed winding number, the solutions can also be indexed in a finite number of branches classified by the mass and the non-Abelian magnetic charge. These branches generally follow the picture found for $n = 1$ (with higher values of mass, however). This is in sharp contrast to the $\Lambda = 0$ case, where only a discrete set of solutions is found [23]. Also, the Kretschman scalar $K = R_{ijkl}R^{ijkl}$ remains finite for every $(r \geq r_h, \theta)$.

It is rather difficult to find some general pattern valid for every considered configuration. Qualitatively, the YM field behavior is similar to that corresponding to solutions in a fixed SAdS background. We notice a similar shape for the functions H_i and also for the energy density. Similar to $n = 1$ case, as long as the YM energy contribution is small enough (the integral (59) is much smaller than the total mass), the YM solutions in a fixed SAdS background give a good approximation to a solution of the EYM equations. Again, for large enough values of $|\Lambda|$, the derivation of the functions H_2 and H_4 from the event horizon value is very small.

The gauge functions H_2, H_3, H_4 start always at (angle dependent) nonzero values on the event horizon. The general picture presented in Fig. 2 is valid in this case too. Starting with suitable $n = 1$ configurations, we find both solutions where H_2, H_4 cross the r axis and nodeless solutions. The gauge function H_2 is always almost spherically symmetric, while the gauge functions H_1 and H_3 are about one order of magnitude smaller than the functions H_2 and H_4.

For the considered solutions, the metric functions m, f, l do not exhibit a strong angular dependence. These functions start with a zero value on the event horizon and approach rapidly the asymptotic values. We have also observed little dependence of the metric functions on the node number. The functions m and l have a rather similar shape, while the ratio m/l indicating the deviation from spherical symmetry is typically close to one, except in a region near the horizon.

However, we found that, similar to the asymptotically flat case, the horizon is deformed. This deformation is parametrized by the ratio L_e/L_p, where L_e is the circumference measured along the equator and L_p is the circumference measured along the poles

$$L_e = \int_0^{2\pi} d\varphi \left. \sqrt{\frac{l}{f}} r \sin\theta \right|_{r=r_h,\theta=\pi/2} = 2\pi r_h \left. \sqrt{\frac{l_2}{f_2}} \right|_{\theta=\pi/2} , \qquad (76)$$

$$L_p = 2 \int_0^\pi d\theta \left. \sqrt{\frac{m}{f}} r \right|_{r=r_h,\varphi=const.} = 2r_h \int_0^\pi d\theta \sqrt{\frac{m_2(\theta)}{f_2(\theta)}} . \qquad (77)$$

For most of the considered solutions, this derivation from spherical symmetry is very small, however, at the limit of the numerical errors. We have found typically $L_e/L_p \simeq 0.99$ (although the situation may be different for other values of the event horizon radius). Similar to the static asymptotically flat case, it remains a challenge to construct static solutions with a large horizon deformation.

To see the the winding number dependence for a fixed magnetic charge, we present in Fig. 7 three solutions with $\omega_0 = 1.73$ and $n = 1, 2$ and 3. In Figs. 7a-d the gauge field functions are shown, in Figs. 7e-g the metric functions, and in Fig. 7h the energy density of the matter fields. These two-dimensional plots exhibit the r dependence for three angles $\theta = 0$, $\pi/4$ and $\pi/2$. Note that for $\omega_0 > 1$ the H_1, H_3 functions remain nodeless (H_1 and H_3 are zero on the axes in Figs. 7a,c as required by the boundary conditions (18)). As expected, the angular dependence of the matter functions increases with the winding number n and the location of the biggest angular splitting moves further outward. Also, we can see that for every

n, the global maximum of the energy density for these black hole solutions resides on the $z-$axis at the event horizon, while a pronounced minimum develops on the $\rho-$axis at the horizon. However, this is not a generic property and we expect the situation to be different for smaller values of r_h and the same Λ, ω_0. In fact, even for $r_h = 1$ we have found configurations with a maximum of the energy density along the ρ axis.

In Figure 8 the mass M of this branch of black hole solutions is plotted as a function of the nonabelian magnetic charge Q_M for various winding numbers. These solutions have been obtained for a cosmological constant $\Lambda = -0.1$. For an event horizon radius $r_h = 1$, this value is of interest because the corresponding solutions combine basic features of the small $|\Lambda|$ case (with a large number of branches and node number $k \geq 0$) and large $|\Lambda|$ case (one branch and nodeless solutions only). For $\Lambda = -0.1$ and $n \geq 1$ and we find one branch of solutions with both nodeless ($\omega_0 > 0$) and one-node configurations (with ω_0 taking negative values up to $\omega_0^{min} \simeq -0.155$ and extending backwards to zero). Note also that for the physically more interesting value $\Lambda = -3$, the black hole configurations with $r_h = 1$ present only one branch of nodeless solutions, with very small variations of the gauge fields outside the event horizon. A detailed analysis of the static black hole solutions as well as rotating regular solutions with $\Lambda = -3$, will be presented elsewhere in connection to the $d = 11$ supergravity embedding.

Figure 9a shows a typical three-dimensional plot of the T_t^t component of the energy-momentum tensor as a function of the coordinates ρ and z, for a black hole solution with $r_h = 1$, $\Lambda = -1$, $Q_M = 1.52$, $n = 2$ and $k = 0$. In Figures 9b-d surfaces of constant energy density are presented for the same solution. As expected, the energy density is not constant at the horizon but angle dependent. Similar to the asymptotically flat case, the surfaces of constant energy density appear ellipsoidal for small values of ϵ, being flatter at the poles than in the equatorial plane. With increasing values of ϵ, a torus-like shape appears, with the horizon seen at the center of the torus. We did not observe a strong dependence of this picture on the value of the cosmological constant.

To illustrate the dependence of the black hole solutions on the value of the cosmological constant, we show in Fig. 10 three $n = 2$ solutions with the same magnetic charge $Q_M = 1.52$, obtained for different values of Λ. In Figs. 10a-d the gauge field functions are presented, in Figs. 10e-g the metric functions, and in Fig. 10h the energy density $-T_t^t$. We can notice that, for increasing $|\Lambda|$, the metric functions approach the asymptotic values faster than in the limit of small cosmological constant, as the magnetic field concentrates near the event horizon. Given n, ω_0, r_h, by decreasing the cosmological constant from 0 to $-\infty$, the field variables decrease for fixed r. However, the angular dependence of the metric and matter functions does not change significantly with $|\Lambda|$ (although the angular dependence of the matter variables on the event horizon increases). The peak of the energy density shifts inward with increasing $|\Lambda|$ and increases in height.

The mass-temperature diagrams for black hole monopole solutions at $\Lambda = -0.1$, $r_h = 1$ and three winding numbers are plotted in Figure 11. The magnetic potential at infinity ω_0 varies along each curve. The higher branches in this picture corresponds to values of $\omega_0 < 1$, while $\omega_0 > 1$ for the lower branches. The common point of these curves corresponds to the SAdS solution with $\omega_0 = 1$ [4]. Thus, it seems that the Hawking temperature of a EYM system appears to be suppressed relative to that of a vacuum black hole of equal horizon area (this result can be proven analytically for $n = 1$ only [21]), while the mass always increases.

We don't address here the problem of limiting solutions, which is still unclear even in the spherically symmetric case. Axially symmetric generalizations of the spherically symmetric configurations near the critical solutions are difficult to obtain, with large errors for the gauge functions H_1 and H_3.

6 CONCLUSIONS

In this paper we have presented numerical arguments that EYM theory with a negative cosmological constant possesses black hole static axially symmetric solutions. These static configurations are asymptotically

---

[4]For any value of n, the solution with $\omega_0 = 1$ corresponds to a trivial gauge configuration with $H_1 = H_3 = 0$, $H_2 = H_4 = 1$ i.e. $F_{\mu\nu} = 0$ and a SAdS geometry.

AdS, possesing a regular event horizon. They generalize to higher winding number the known spherically symmetric solutions, presenting angle-dependent fields at the horizon.

We started by presenting arguments that YM-SU(2) theory possess solutions with nonvanishing magnetic and electric charges and arbitrary winding number for a SAdS black hole fixed background. The spherically symmetric solutions we found have properties similar to the lower branch of their known gravitating counterparts. Axially symmetric YM configurations with nonzero electric potentials have been considered as well, some of them presenting a nonvanishing total angular momentum.

When including gravity, we have presented results suggesting the existence of axially symmetric EYM black hole solutions with negative cosmological constant. Like their regular counterparts, these black hole configurations have continuous values of mass and non-Abelian magnetic charge and present a branch structure.

We have not considered the question of stability for higher winding number solutions. However, since some of the static spherically symmetric black hole solutions are stable [10], there is all reason to believe, that there are also static axially symmetric black stable against small time-dependent perturbations. A rigorous proof is however desirable, analogous to the proof given for the spherically symmetric case.

Axially symmetric EYM solutions with a different topology of the event horizon, generalizing for $n > 1$ the known topological black holes [21] are also likely to exist. Rotating configurations should exist as well, leading to nonabelian counterparts of the Kerr-Newman-AdS abelian solution. Here we expect the situation to be more complicated as compared to the asymptotically flat case. For $\Lambda \neq 0$ the boundary solutions in the asymptotic region are less restrictive allowing for a nonvanishing value of the electric potential at infinity which complicates the general picture.

In fact we expect all known asymptotically flat configurations to generalize for a negative cosmological constant. It would be interesting to construct AAdS nonabelian solutions which possess only discrete symmetries [51] and to find the corresponding boundary stress tensor. Their interpretation in AdS/CFT context is a challange.

Acknowledgements

References

[1] S. W. Hawking and D. N. Page, Commun. Math. Phys. **87** (1983) 577.

[2] E. Witten, Adv. Theor. Math. Phys. **2** (1998) 253 [arXiv:hep-th/9802150].

[3] J. M. Maldacena, Adv. Theor. Math. Phys. **2** (1998) 231 [Int. J. Theor. Phys. **38** (1999) 1113] [arXiv:hep-th/9711200].

[4] E. Witten, Adv. Theor. Math. Phys. **2** (1998) 505 [arXiv:hep-th/9803131].

[5] A. Chamblin, R. Emparan, C. V. Johnson and R. C. Myers, Phys. Rev. D **60** (1999) 064018 [arXiv:hep-th/9902170];
A. Chamblin, R. Emparan, C. V. Johnson and R. C. Myers, Phys. Rev. D **60** (1999) 104026 [arXiv:hep-th/9904197].

[6] R. B. Mann, arXiv:gr-qc/9709039;
J. P. Lemos, arXiv:gr-qc/0011092.

[7] E. Winstanley, Found. Phys. **33** (2003) 111 [arXiv:gr-qc/0205092].

[8] M. H. Dehghani, A. M. Ghezelbash and R. B. Mann, Phys. Rev. D **65** (2002) 044010 [arXiv:hep-th/0107224].

[9] M. H. Dehghani and T. Jalali, Phys. Rev. D **66** (2002) 124014 [arXiv:hep-th/0209124].

[10] E. Winstanley, Class. Quant. Grav. **16** (1999) 1963 [arXiv:gr-qc/9812064].

[11] J. Bjoraker and Y. Hosotani, Phys. Rev. D **62** (2000) 043513 [arXiv:hep-th/0002098].

[12] A. R. Lugo and F. A. Schaposnik, Phys. Lett. B **467** (1999) 43 [arXiv:hep-th/9909226].

[13] A. R. Lugo, E. F. Moreno and F. A. Schaposnik, Phys. Lett. B **473** (2000) 35 [arXiv:hep-th/9911209].

[14] J. J. van der Bij and E. Radu, Int. J. Mod. Phys. A **18** (2003) 2379 [arXiv:hep-th/0210185].

[15] O. Sarbach and E. Winstanley, Class. Quant. Grav. **18** (2001) 2125 [arXiv:gr-qc/0102033].

[16] P. Breitenlohner, D. Maison and G. Lavrelashvili, Class. Quant. Grav. **21** (2004) 1667 [arXiv:gr-qc/0307029].

[17] E. Radu, Phys. Rev. D **67** (2003) 084030 [arXiv:hep-th/0211120].

[18] N. Okuyama and K. i. Maeda, Phys. Rev. D **67** (2003) 104012 [arXiv:gr-qc/0212022].

[19] E. Radu, Phys. Lett. B **548** (2002) 224 [arXiv:gr-qc/0210074].

[20] E. Radu, Phys. Rev. D **65** (2002) 044005 [arXiv:gr-qc/0109015].

[21] J. J. Van der Bij and E. Radu, Phys. Lett. B **536** (2002) 107 [arXiv:gr-qc/0107065].

[22] B. Kleihaus and J. Kunz, Phys. Rev. Lett. **79** (1997) 1595 [arXiv:gr-qc/9704060].

[23] B. Kleihaus and J. Kunz, Phys. Rev. D **57** (1998) 6138 [arXiv:gr-qc/9712086].

[24] M. S. Volkov and D. V. Galtsov, Sov. J. Nucl. Phys. **51** (1990) 747 [Yad. Fiz. **51** (1990) 1171];
P. Bizon, Phys. Rev. Lett. **64** (1990) 2844;
H. P. Kuenzle and A. K. M. Masood- ul- Alam, J. Math. Phys. **31** (1990) 928.

[25] B. Kleihaus and J. Kunz, Phys. Rev. D **57** (1998) 834 [arXiv:gr-qc/9707045].

[26] B. Kleihaus, J. Kunz and F. Navarro-Lerida, Phys. Rev. D **66** (2002) 104001 [arXiv:gr-qc/0207042].

[27] C. N. Pope, Class. Quant. Grav. **2** (1985) L77.

[28] G. W. Gibbons and S. W. Hawking, Phys. Rev. D **15** (1977) 2752.

[29] N. S. Manton, Nucl. Phys. B **135** (1978) 319.

[30] C. Rebbi and P. Rossi, Phys. Rev. D **22** (1980) 2010.

[31] P. Forgacs and N. S. Manton, Commun. Math. Phys. **72** (1980) 15;
P. G. Bergmann and E. J. Flaherty, J. Math. Phys. **19** (1978) 212.

[32] B. Kleihaus and J. Kunz, Phys. Rev. D **61** 025003 (2000) [hep-th/9909037];
Y. Brihaye and J. Kunz, Phys. Rev. D **50**, 4175 (1994) [hep-ph/9403392];
B. Kleihaus and J. Kunz, Phys. Rev. D **50** 5343 (1994) [hep-ph/9405387].

[33] D. Kramer, H. Stephani, E. Herlt, and M. MacCallum, Exact Solutions of Einstein's Field Equations, Chapter 17, Cambridge University Press, Cambridge, (1980).

[34] B. Hartmann, B. Kleihaus and J. Kunz, Phys. Rev. D **65** (2002) 024027 [arXiv:hep-th/0108129].

[35] L. F. Abbott and S. Deser, Nucl. Phys. B **195** 76 (1982).

[36] M. Henneaux and C. Teitelboim, Commun. Math. Phys. **98** 391 (1985).

[37] V. Balasubramanian and P. Kraus, Commun. Math. Phys. **208** (1999) 413 [arXiv:hep-th/9902121].

[38] M. M. Taylor-Robinson, arXiv:hep-th/0002125.

[39] R. C. Myers, Phys. Rev. D **60** (1999) 046002.

[40] H. Lu and J. F. Vazquez-Poritz, arXiv:hep-th/0308104.

[41] R. B. Mann, Found. Phys. **33** (2003) 65 [arXiv:gr-qc/0211047].

[42] A. Corichi and D. Sudarsky, Phys. Rev. D **61** (2000) 101501 [arXiv:gr-qc/9912032];
A. Corichi, U. Nucamendi and D. Sudarsky, Phys. Rev. D **62** (2000) 044046 [arXiv:gr-qc/0002078].

[43] H. Boutaleb-Joutei, A. Chakrabarti and A. Comtet, Phys. Rev. D **20** 1884 (1979).

[44] Y. Hosotani, J. Math. Phys. **43** (2002) 597 [arXiv:gr-qc/0103069].

[45] P. Bizon, Acta Phys. Polon. B **25** (1994) 877 [arXiv:gr-qc/9402016].

[46] W. Schönauer and R. Weiß, J. Comput. Appl. Math. **27**, 279 (1989);
M. Schauder, R. Weiß and W. Schönauer, The CADSOL Program Package, Universität Karlsruhe,
Interner Bericht Nr. 46/92 (1992);
W. Schönauer and E. Schnepf, ACM Trans. on Math. Soft. **13**, 333 (1987).

[47] P. Bizon, O.T. Popp, Class. Quant. Grav. **9** 193 (1992);
A.A. Ershov, D.V. Galtsov, Phys. Lett. **A150** 159 (1990).

[48] B. Hartmann, B. Kleihaus and J. Kunz, Mod. Phys. Lett. A **15** (2000) 1003 [arXiv:hep-th/0004108].

[49] D. Sudarsky, R. M. Wald, Phys.Rev. **D46** 1453 (1992).

[50] J. J. Van der Bij and E. Radu, Int. J. Mod. Phys. A **17** (2002) 1477 [arXiv:gr-qc/0111046].

[51] B. Kleihaus, J. Kunz and K. Myklevoll, Phys. Lett. B **582**, 187 (2004) [arXiv:hep-th/0310300].

Appendix

We consider spacetimes whose metric can be written locally in the form

$$ds^2 = e^{2C(r)}dr^2 + e^{2A(r)-2B(r)}d\Omega_k^2 - e^{2B(r)}dt^2, \tag{78}$$

where $d\Omega_k^2 = d\theta^2 + f^2(\theta)d\varphi^2$ is the metric on a two-dimensional surface of constant curvature $2k$. The discrete parameter k takes the values $1, 0$ and -1 and implies the form of the function $f(\theta)$

$$f(\theta) = \begin{cases} \sin\theta, & \text{for } k = 1 \\ \theta, & \text{for } k = 0 \\ \sinh\theta, & \text{for } k = -1. \end{cases} \tag{79}$$

In these solutions, the topology of the two-dimensional space $t = const.$, $r = const.$ depends on the value of k. When $k = 1$, the metric takes on the familiar spherically symmetric form, for $k = -1$ the (θ, φ) sector is a space with constant negative curvature (also known as a hyperbolic plane), while for $k = 0$, this is a flat surface. For any value of k, the metric (78) has four Killing vectors, one timelike and three spacelike.

The most general expression for the appropriate SU(2) connection is obtained by using the standard rule for calculating the gauge potentials for any spacetime group [31]. Taking into account the symmetries of the line element (78) we find [21]

$$A = \frac{1}{2g}\left\{u(r,t)\tau_3 dt + \chi(r,t)\tau_3 dr + (\omega(r,t)\tau_1 + \tilde{\omega}(r,t)\tau_2)\, d\theta + \left(\frac{d\ln f}{d\theta}\tau_3 + \omega(r,t)\tau_2 - \tilde{\omega}(r,t)\tau_1\right)fd\varphi\right\}. \quad (80)$$

For purely magnetic, static configurations (*i.e.* $u = 0$) it is convenient to take the $\chi = 0$ gauge and eliminate $\tilde{\omega}$ by using a residual gauge freedom. The remaining function ω depends only on the coordinate r. As a result, we obtain the YM curvature

$$F = \frac{1}{2g}\left(\omega'\tau_1 dr \wedge d\theta + f\omega'\tau_2 dr \wedge d\varphi + (w^2 - k)f\tau_3 d\theta \wedge d\varphi\right), \quad (81)$$

where a prime denotes a derivative with respect to r.

Inserting this ansatz into the action (1), integrating and dropping the surface term, we find that the equations of motion can be derived from an effective action whose Lagrangian is given by (the dependence on the coupling constants G, e is eliminated by taking the rescaling (21))

$$L = G_{ik}(y)\frac{dy^i}{dr}\frac{dy^k}{dr} - U(y), \quad (82)$$

where $y^i = (A, B, \omega)$ and $G_{ik} = e^{2A-B-C}\text{diag}(1, -1, -2e^{-2A+2B})$ and

$$U = -ke^{B+C} + \Lambda e^{2A-B+C} + (\omega^2 - k)^2 e^{-2A+3B+C}. \quad (83)$$

The field equation for the variable C implies the contraint

$$-e^{2A-B-C}(A'^2 - B'^2) + ke^{B+C} + 2\omega'^2 e^{B-C} - \Lambda e^{2A-B+C} - (w^2 - k)^2 e^{-2A+3B+C} = 0. \quad (84)$$

We remark that (82) allows for the reparametrization $r \to \tilde{r}(r)$ which is unbroken by our ansatz.

We are interested in finding a superpotential W such that U to satisfies the relation

$$U = -G^{ik}\frac{\partial W}{\partial y^i}\frac{\partial W}{\partial y^k}, \quad (85)$$

which allows the first order Bogomol'nyi equations

$$\frac{dy^i}{dr} = G^{ik}\frac{\partial W}{\partial y^k}, \quad (86)$$

solving also the second-order EYM equations (3), (5).

In the absence of the YM fields, the superpotential W has the simple form

$$W = \sqrt{ke^{2A} + e^{4A-2B}}, \quad (87)$$

leading to pure-AdS vacuum solutions.

For $\Lambda = -3$ and vanishing curvature ($k = 0$) of the two-dimensional space $r = const.$, $t = const.$, it is possible to find a simple form of the superpotential

$$W_0 = e^B w^2 + e^{2A-B}, \quad (88)$$

leading to a simple solution of the EYM equations. The line element reads

$$ds^2 = dr^2 + \frac{e^{-2r}}{2}(B_0 e^{4r} - \omega_0^2)d\Omega_0^2 - \frac{2e^{6r}}{B_0 e^{4r} - \omega_0^2}dt^2, \quad (89)$$

23

(where ω_0, B_0 are arbitrary real constants; $B_0 > 0$ for a solution with the right signature), while the gauge potential is

$$\omega(r) = \omega_0 e^{-gr}. \tag{90}$$

However, we find that, for every choice of the integration constants, the line element (89) presents some unphysical properties. A direct computation reveals that the point $r = r_0$ (with $e^{4r_0} = \omega_0^2/B_0$) is a curvature singularity (this can easily be seen by computing the invariant $R_{\mu\nu} R^{\mu\nu}$), which is not hidden by an event horizon. As $r \to r_0$, the metric potential g_{tt} diverges, while the other metric functions as well as the gauge field remain finite. Also, the line element (89) approaches asymptotically the AdS background.

Following the rules in [27], this configuration can be uplifted to become a solution of the equations of motion for the $d = 11$ supergravity. Similar solutions are very likely to exist for $k = \pm 1$.
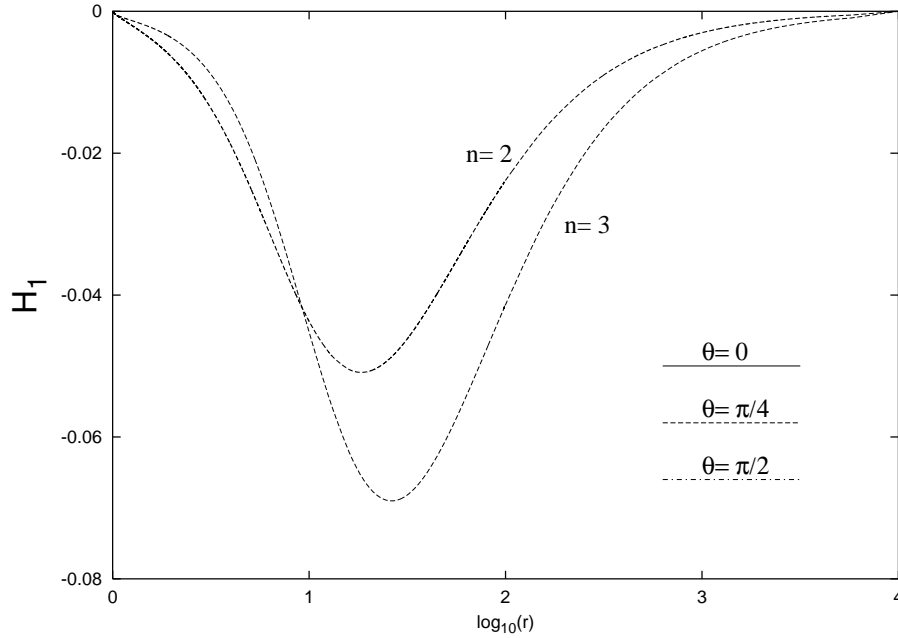
Fig. 1a
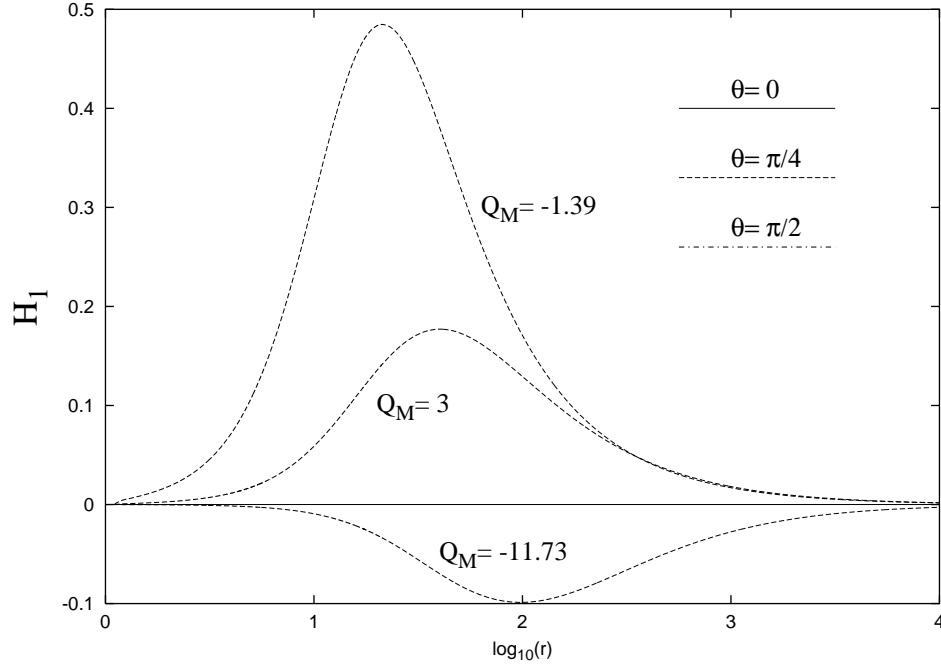
Figure 1a: The gauge function H_1 is shown as a function of the radial coordinate r for the angles $\theta = 0$, $\pi/4$ and $\pi/2$ for three $n = 3$ axially symmetric monopole solutions in a fixed SAdS background with $\Lambda = -0.01$, $r_h = 1$. The magnetic charge and total mass of these YM solutions are ($Q_M = -1.39$, $M = 1.09$), ($Q_M = 3$, $M = 0.33$) and ($Q_M = -11.73$, $M = 0.91$).

Fig. 1b
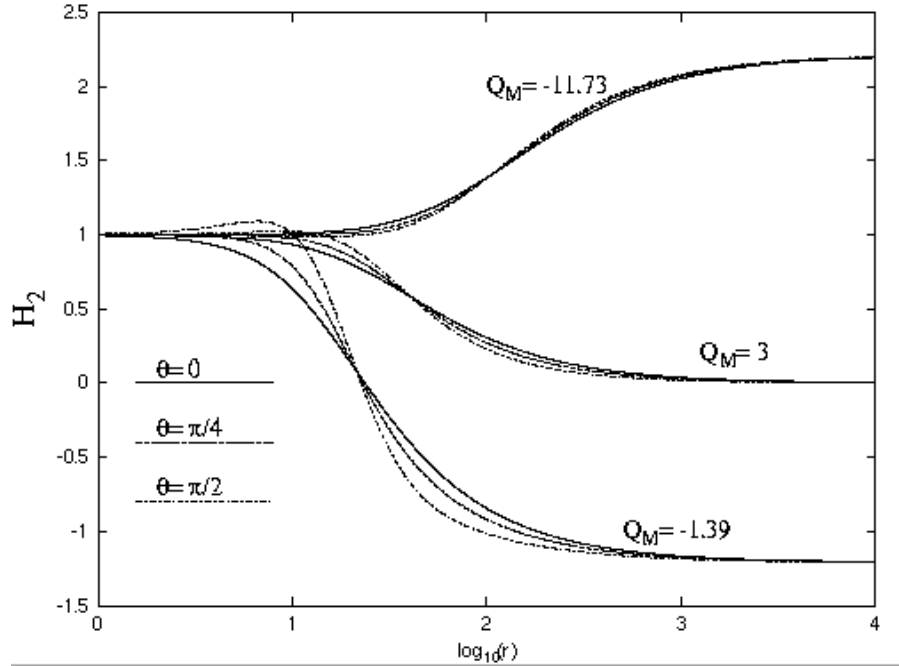
Figure 1b: Same as Fig. 1a for the gauge function H_2.
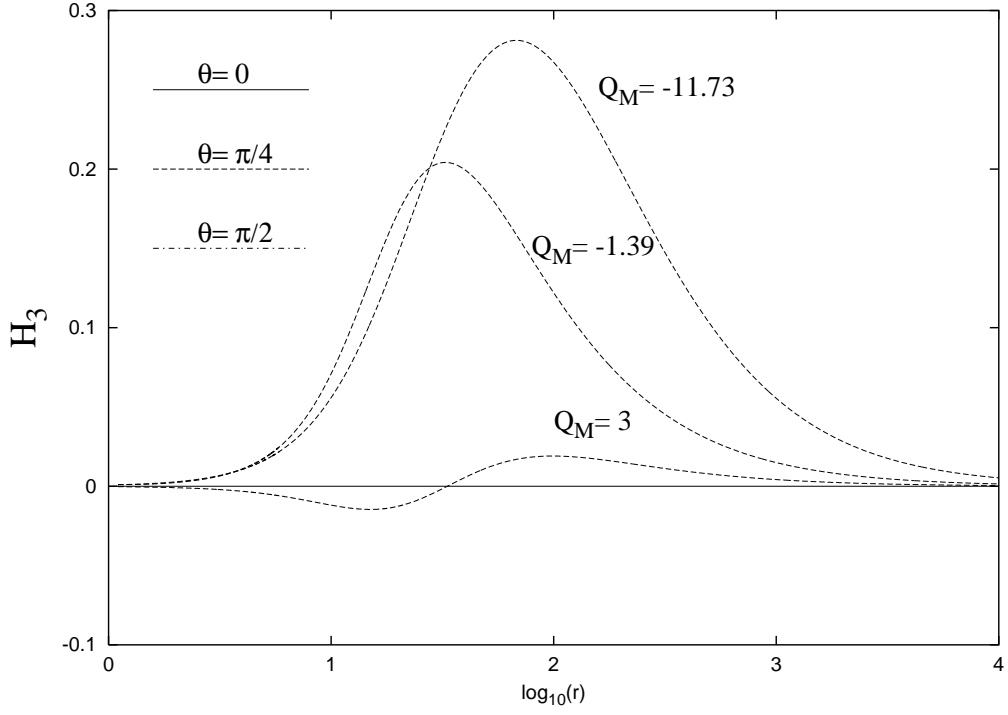
Figure 1c: Same as Fig. 1a for the gauge function H_3.
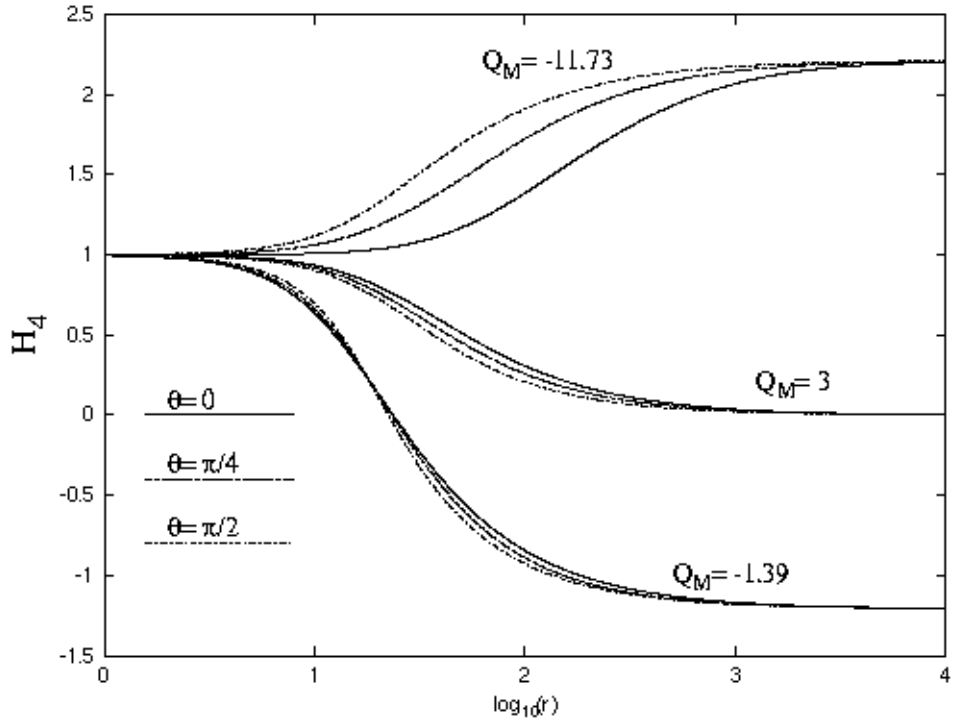
Figure 1d: Same as Fig. 1a for the gauge function H_4.

Fig. 1e
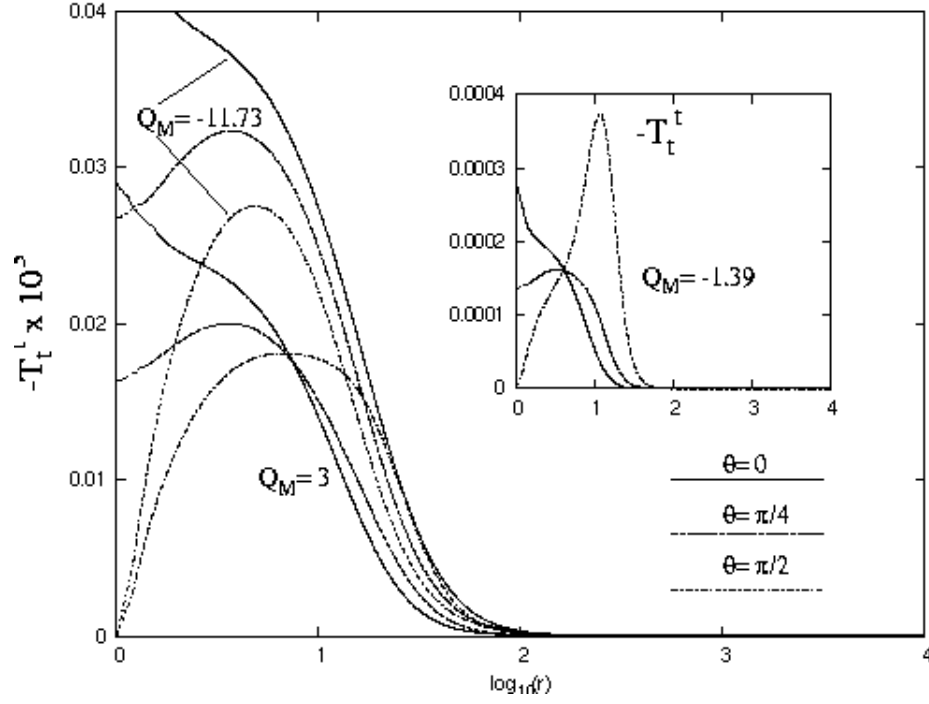
Figure 1e: Same as Fig. 1a for the energy density $-T_t^t$ (in units $4\pi/e^2$).

Fig. 2
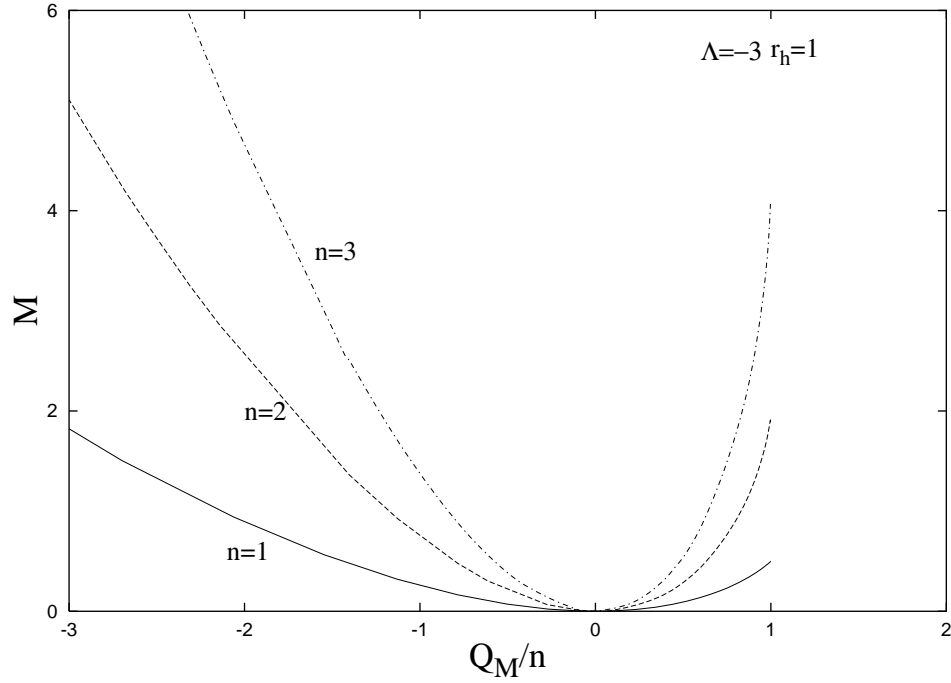
Figure 2: The total mass M (in units $4\pi/e^2$) is plotted as a function of magnetic charge Q_M for monopole solutions in a fixed Schwarzschild-anti de Sitter background with $\Lambda = -3$, $r_h = 1$. The winding number n is also marked.

Fig. 3
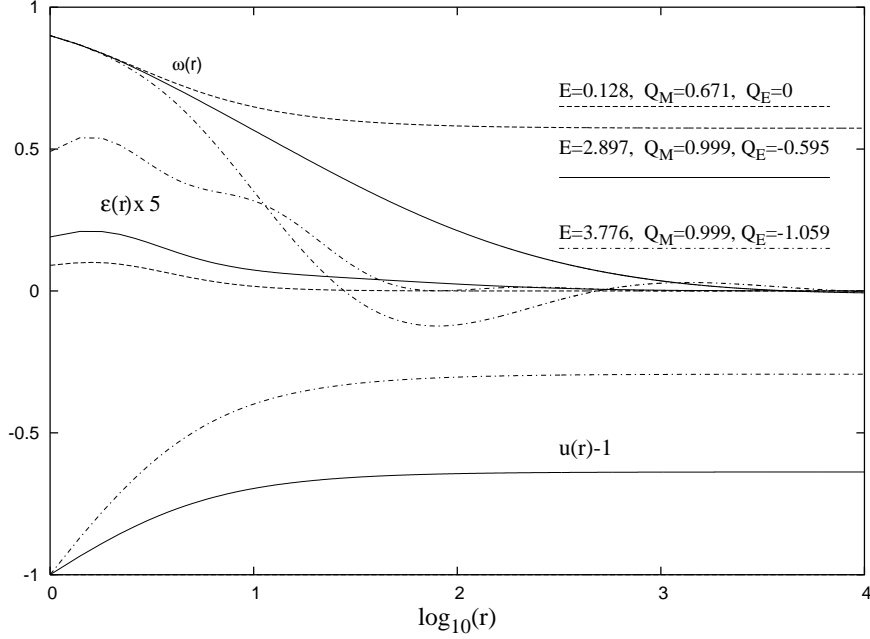
Figure 3: Typical nongravitating spherically symmetric dyon solutions in a SAdS background, for $\Lambda = -1$, $r_h = 1$, the same value of $\omega_h = 0.9$ and $u_h = 0$, 0.2, 0.4. The solution with $u_h = 0$ corresponds to a magnetic monopole. The energy density $\epsilon(r)$ is given in units $4\pi/e^2$.

Fig. 4a
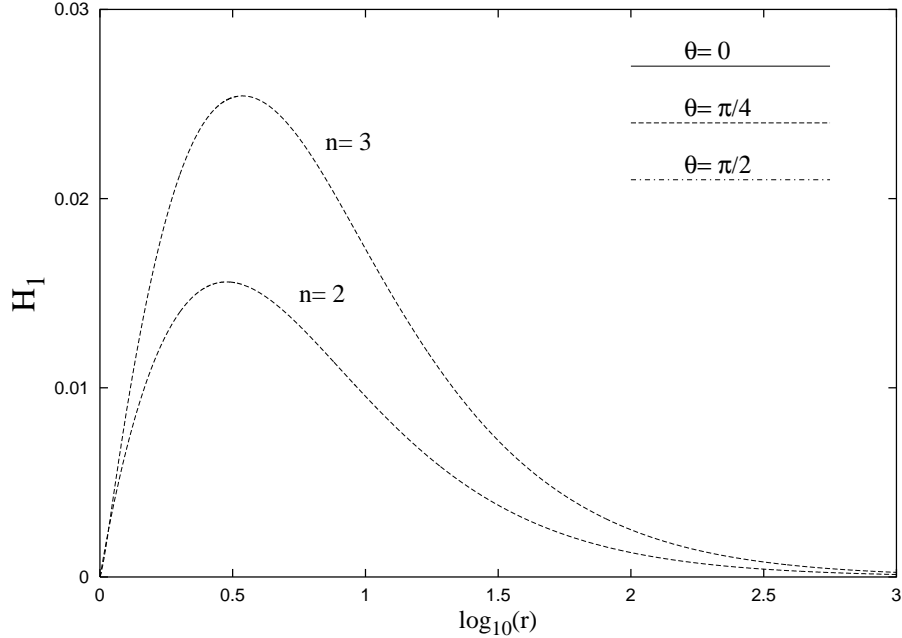
Figure 4a: The gauge function H_1 is shown as a function of the radial coordinate r at $\theta = 0$, $\pi/4$ and $\pi/2$ for three different static dyon solutions. Here the solutions have winding numbers $n = 1$, 2, and 3, the same ratio $Q_M/n = -0.391$, the same value of the electric potential at infinity $u_0 = 0.04$ and masses $M(n = 1) = 1.541$, $M(n = 2) = 1.714$ and $M(n = 3) = 2.071$.

28

Fig. 4b
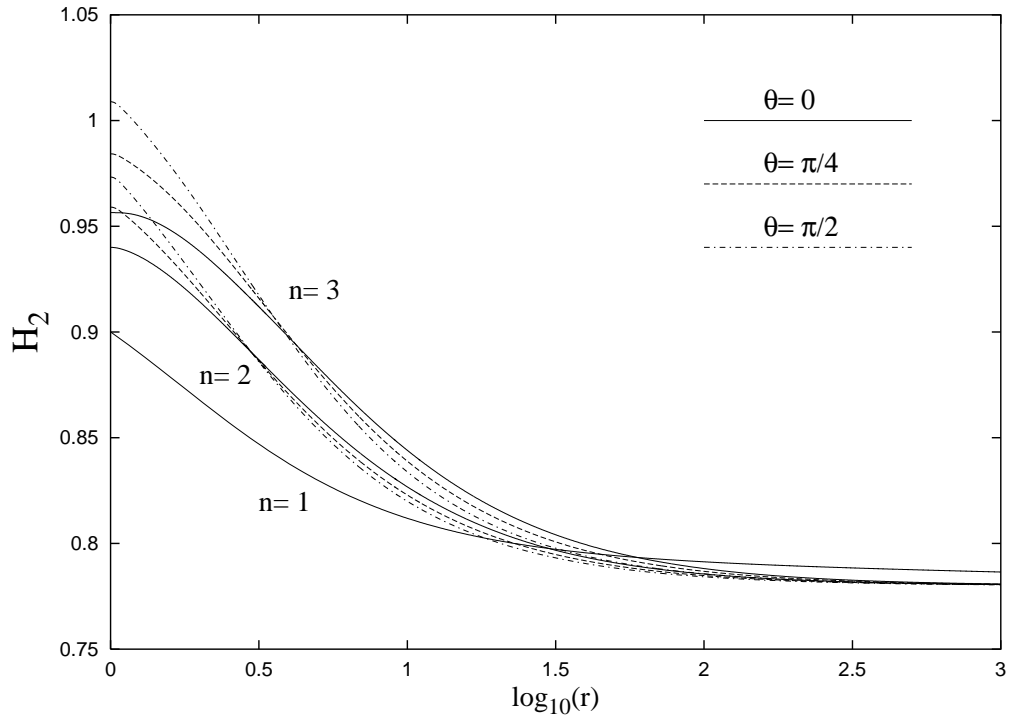
Figure 4b: Same as Fig. 4a for the gauge function H_2.

Fig. 4c
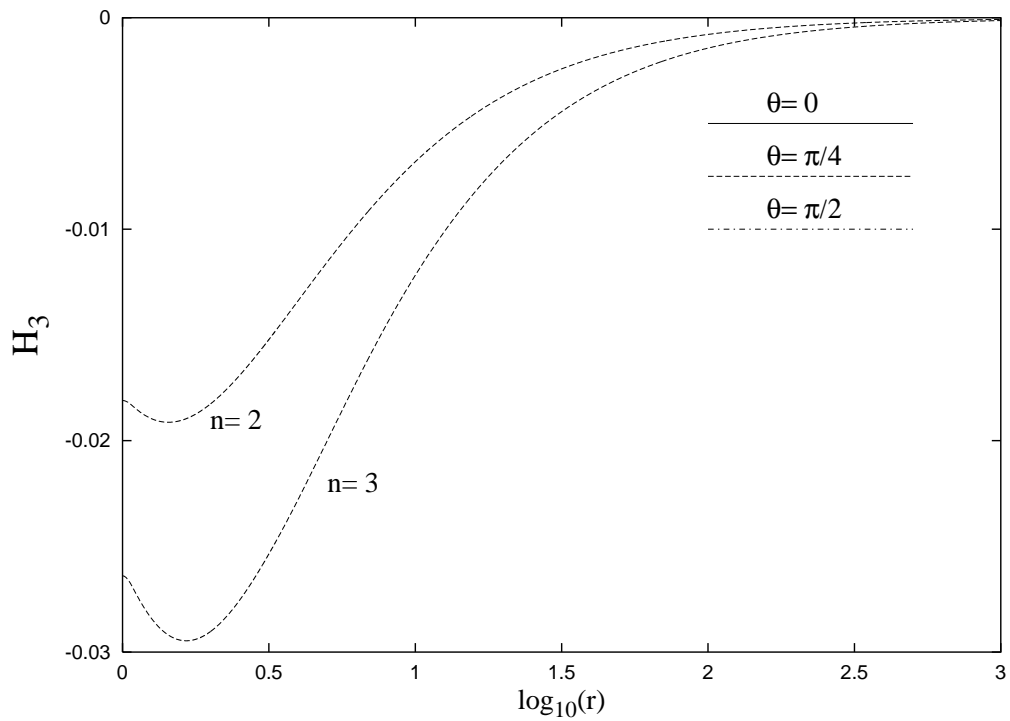
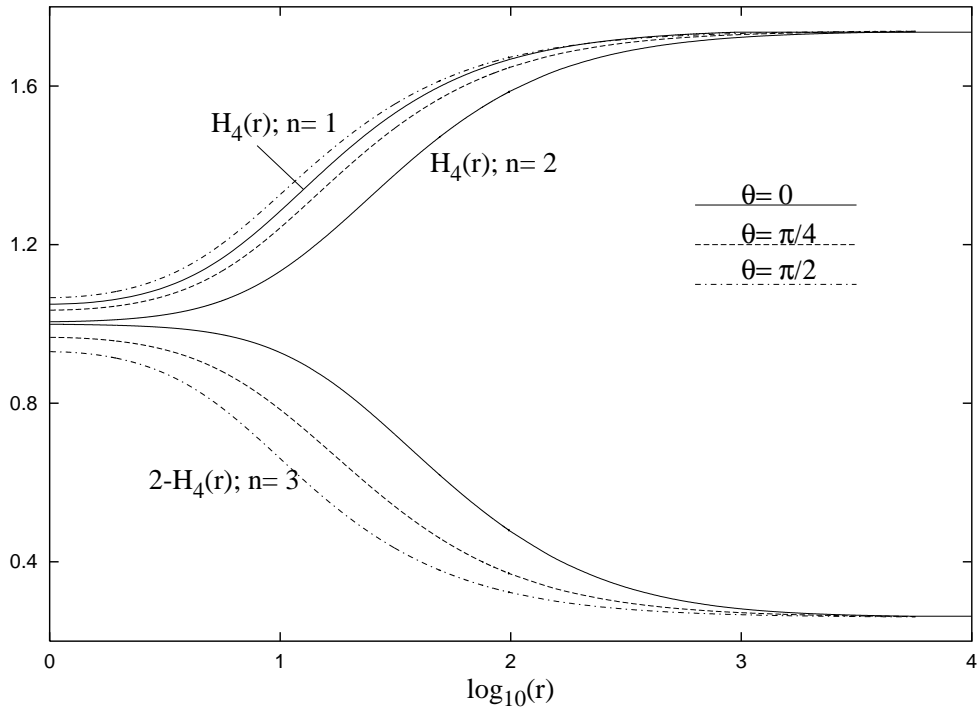Figure 4c: Same as Fig. 4a for the gauge function H_3.

29

Fig. 4d
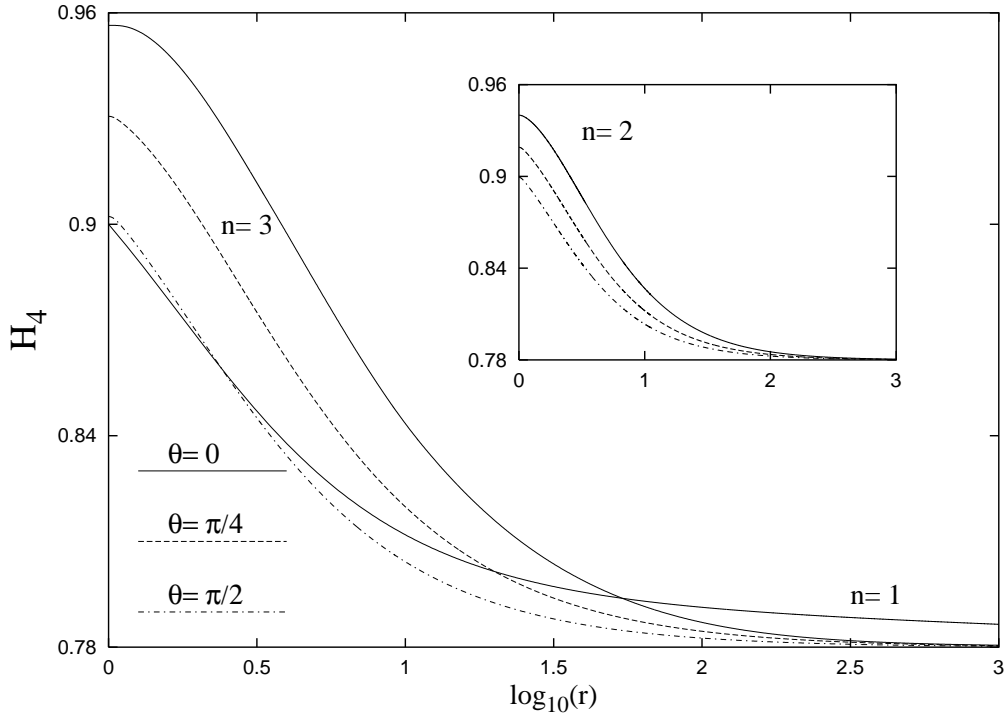
Figure 4d: Same as Fig. 4a for the gauge function H_4.

Fig. 4e
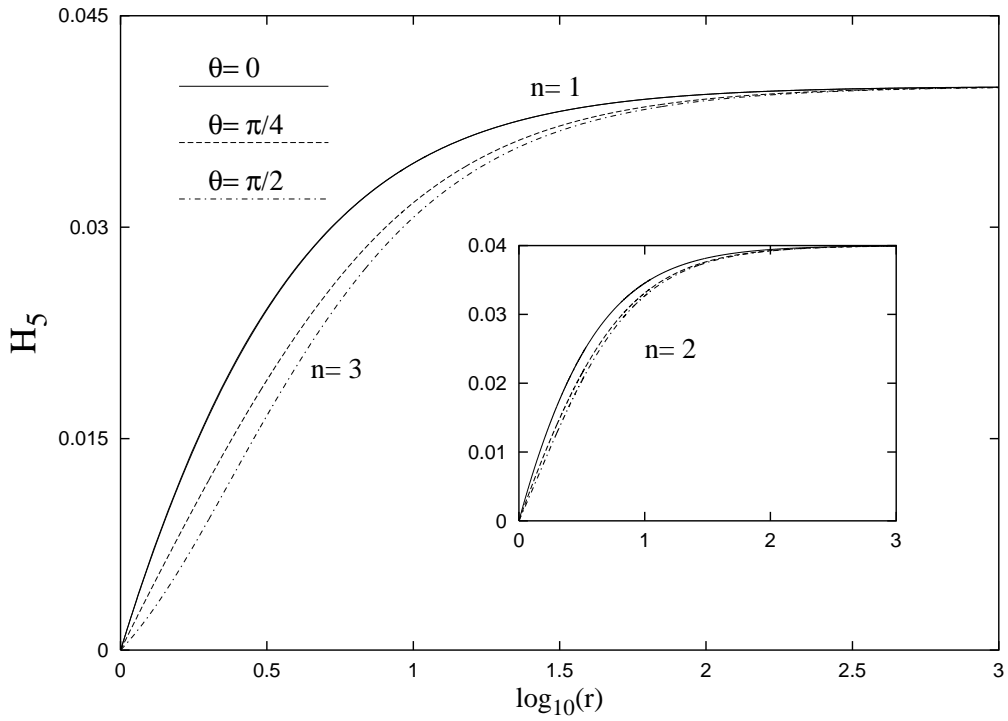
Figure 4e: Same as Fig. 4a for the gauge function H_5.

Fig. 4f
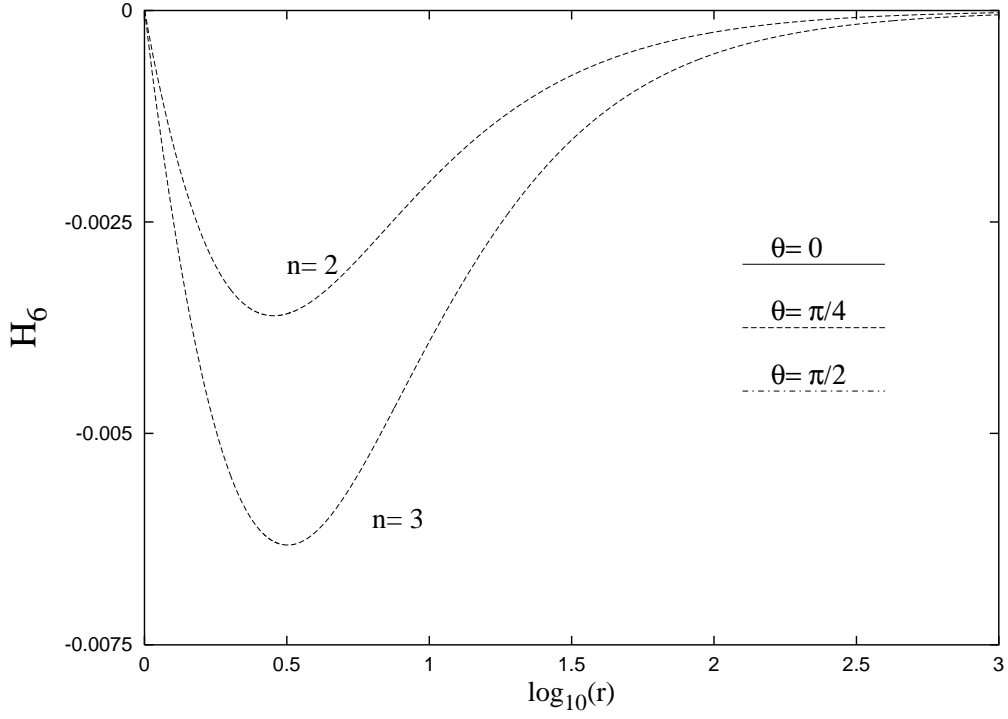
Figure 4f: Same as Fig. 4a for the gauge function H_6.

Fig. 4g
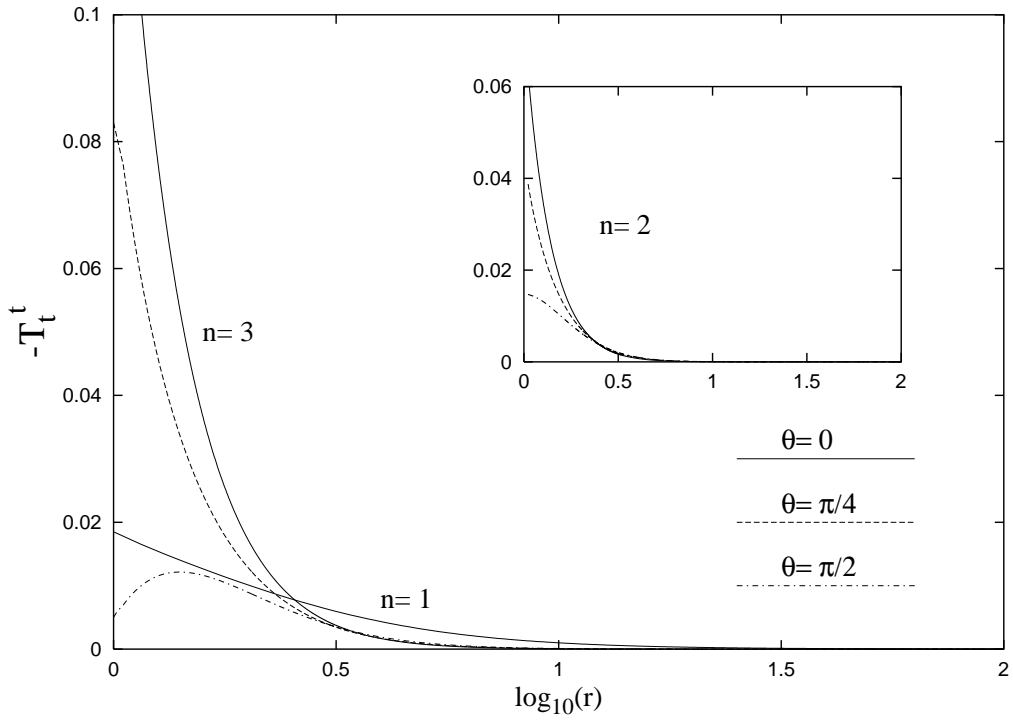
Figure 4g: Same as Fig. 4a for the energy density $\epsilon = -T^t_t$ (in units $4\pi/e^2$).

31

Fig. 5
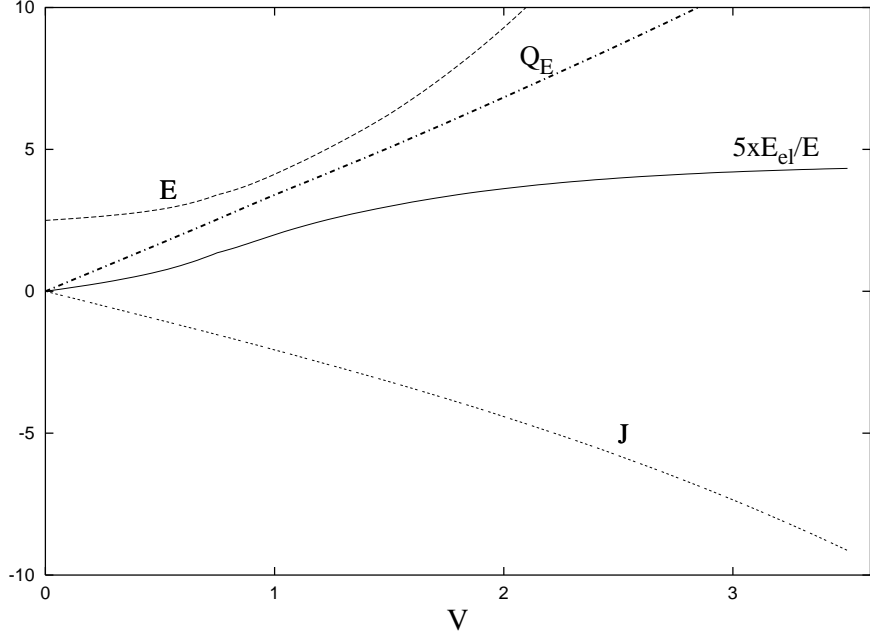
Figure 5: The energy E and the angular momentum J (in units $4\pi/e^2$) for rotating YM dyon solutions in fixed SAdS black hole geometry with $\Lambda = -3$, $r_h = 1$ are shown as a function on the parameter V for a fixed $\omega_0 = 2.15$. Also shown are the electric charge Q_E and the ratio E_e/E.

Fig. 6a
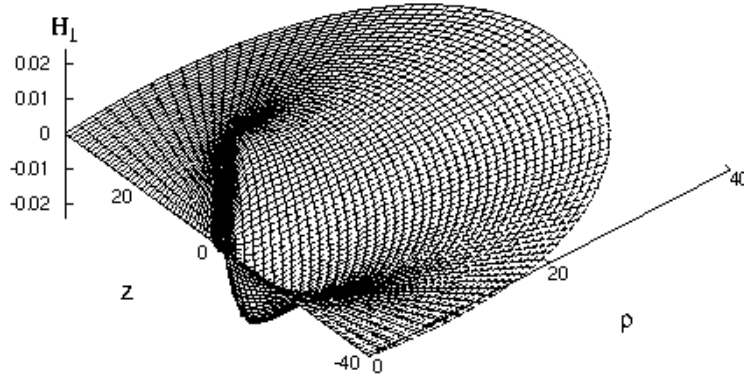
Figure 6a: The magnetic gauge function H_1, is shown as a function of the coordinates $\rho = r\sin\theta$, $z = \rho\cos\theta$ for a rotating dyon solution with $\omega_0 = 2.15$, $V = 2$, $n = 1$. The energy and the angular momentum of this configuration (in units $4\pi/e^2$) are $E = 9.29$ and $J = 4.414$ respectively, while $Q_E = 6.833$. The results are obtained in a SAdS background with $\Lambda = -3$, $r_h = 1$.
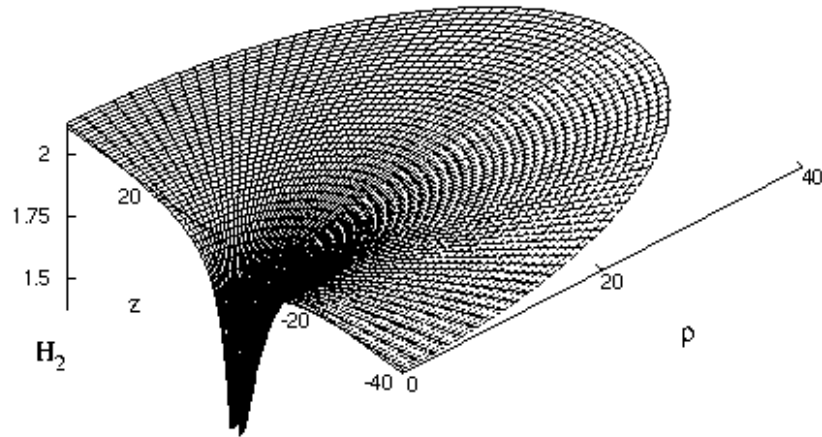
Figure 6b: Same as Fig. 6a for the gauge function H_2.

Fig. 6c
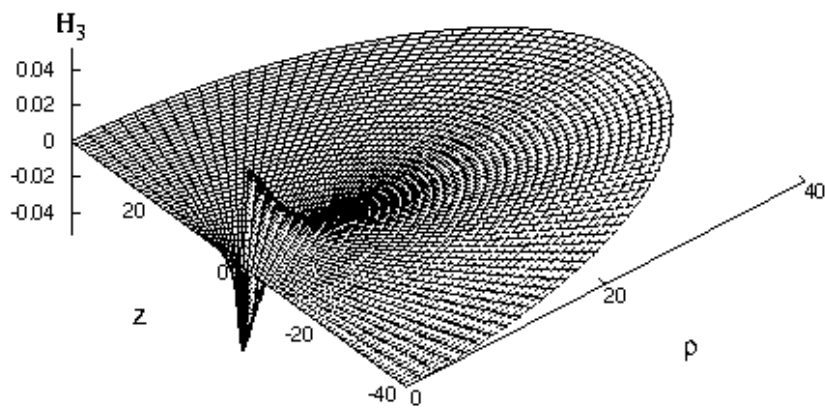
Figure 6c: Same as Fig. 6a for the gauge function H_3.
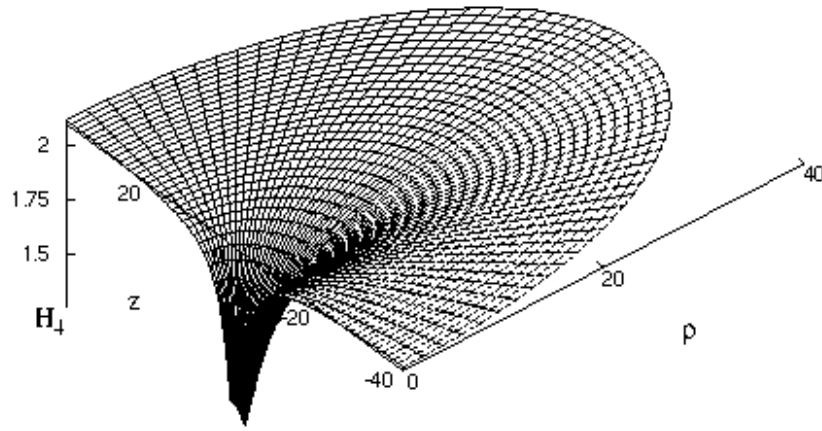
Figure 6d: Same as Fig. 6a for the gauge function H_4.
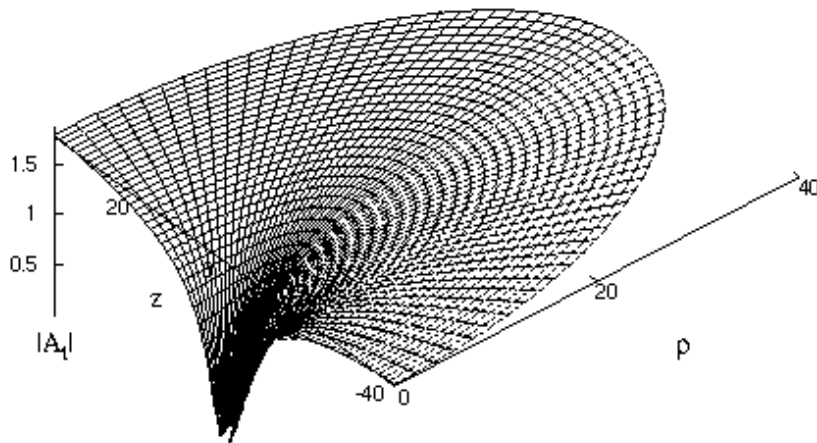
Figure 6e: Same as Fig. 6a for the magnitude of the electric gauge functions $|A_t|$.

Fig. 6f
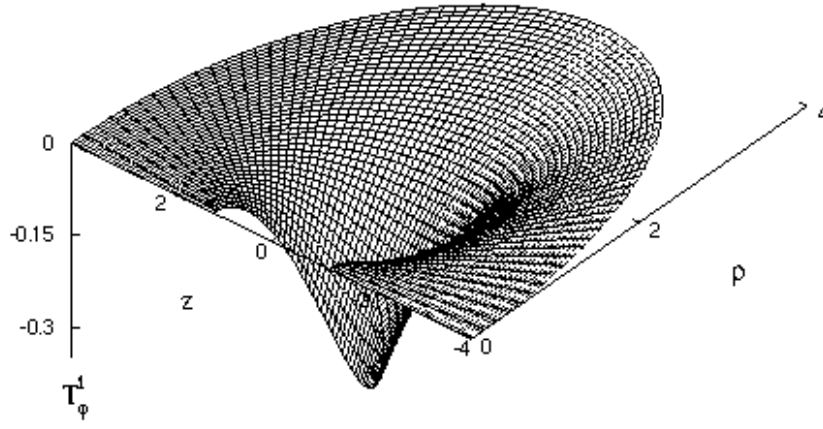
Figure 6f: Same as Fig. 6a for the component T^t_φ of the energy momentum tensor associated with rotation.

Fig. 6g
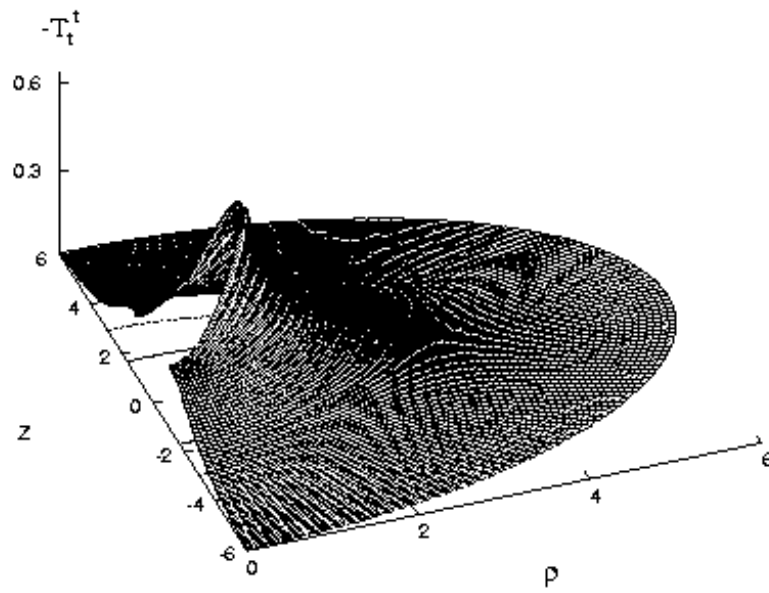
Figure 6g: Same as Fig. 6a for the component T^t_t of the energy momentum tensor.
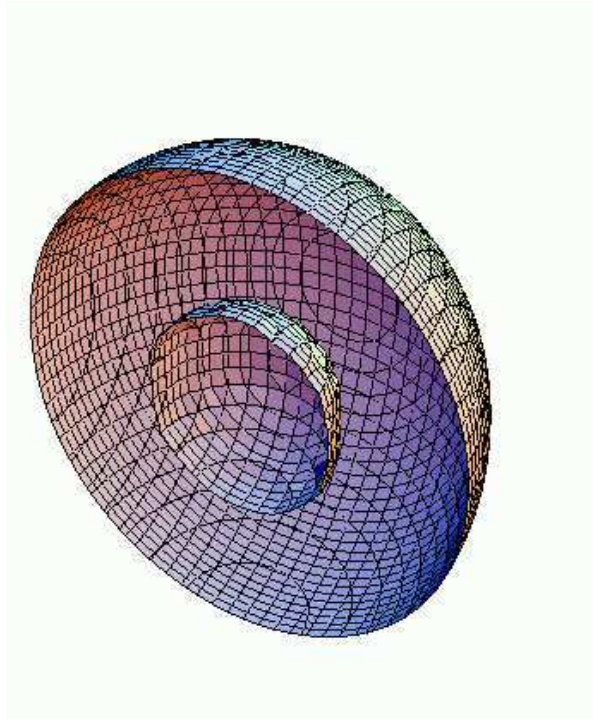
Figure 6h: Surfaces of constant energy density $\epsilon = -T_t^t = 0.16$ are plotted for the same solution.
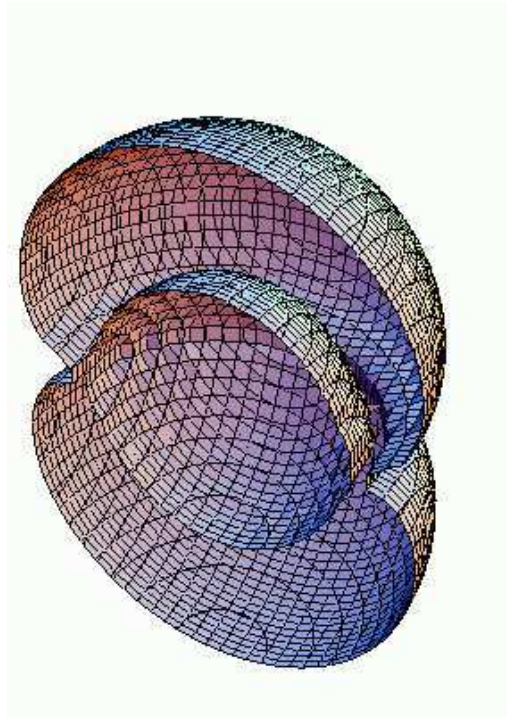
Figure 6i: Same as Fig. 6h for the $\epsilon = -T_t^t = 0.22$.
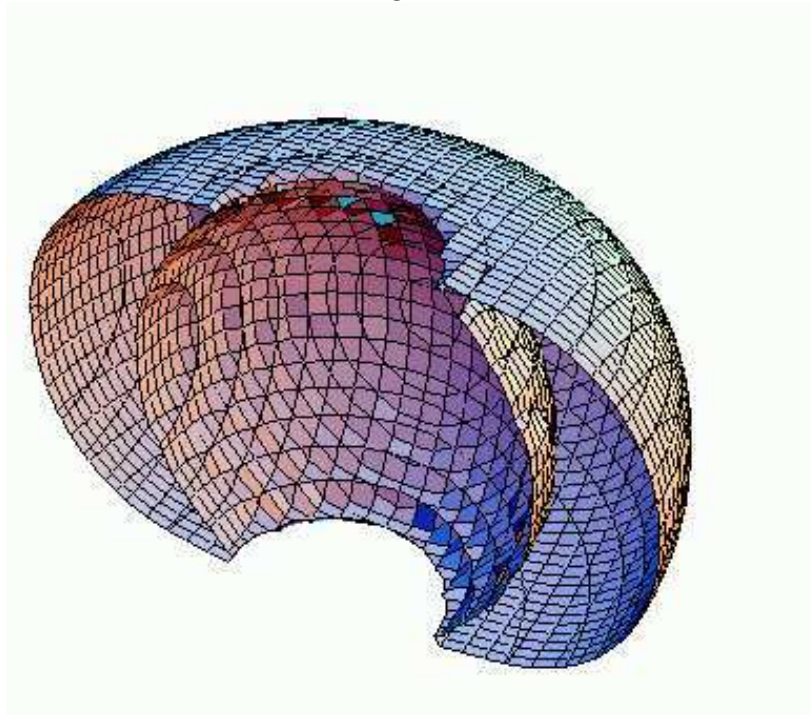
Fig. 6j
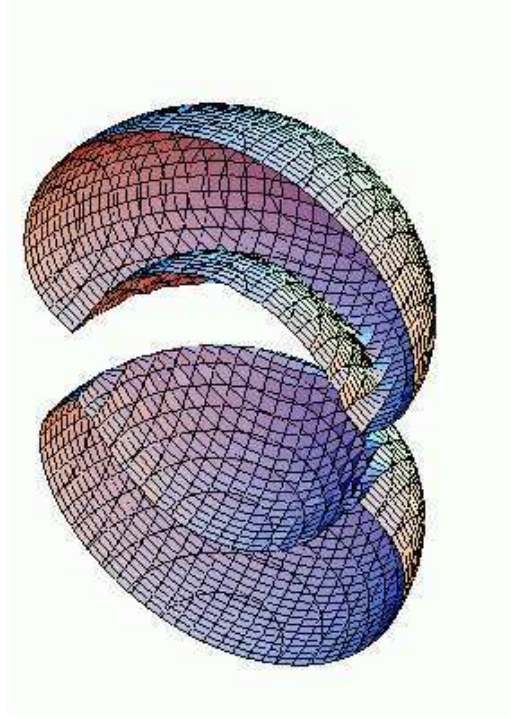
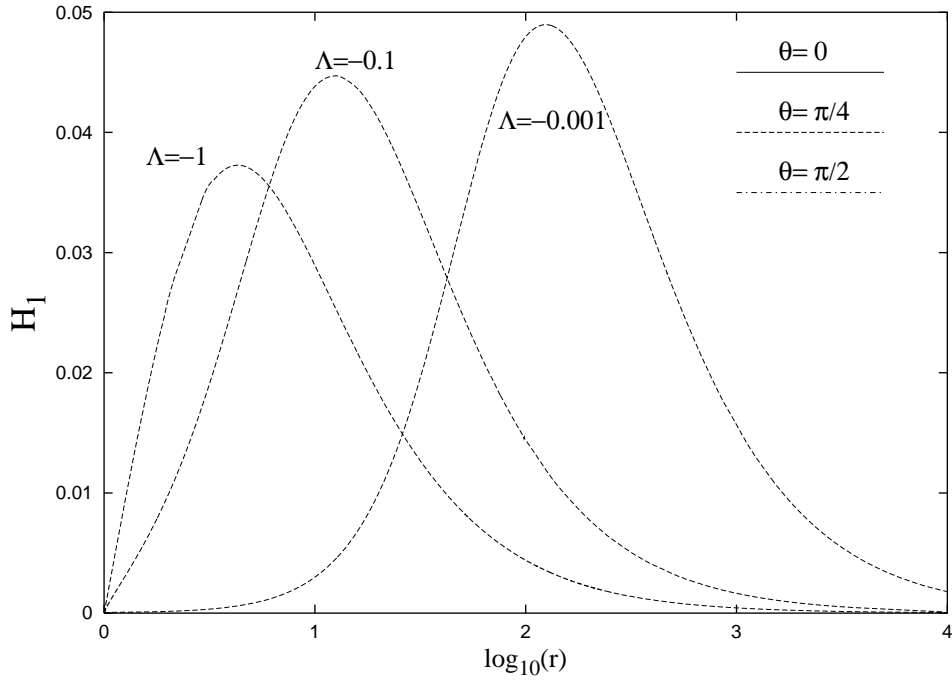Figure 6j: Same as Fig. 6a for the $\epsilon = -T_t^t = 0.24$.

Fig. 7a

Figure 7a: The gauge function H_1 is shown as a function of the radial coordinate r for the angles $\theta = 0$, $\pi/4$ and $\pi/2$. The parameters of these gravitating solutions are: $n = 1$, 2, and 3, $k = 0$, $r_h = 1$, $\Lambda = -0.1$, the node number $k = 0$, $Q_M/n = -2.027$, $M(n = 1) = 1.541$, $M(n = 2) = 1.714$ and $M(n = 3) = 2.071$.

37

Fig. 7b
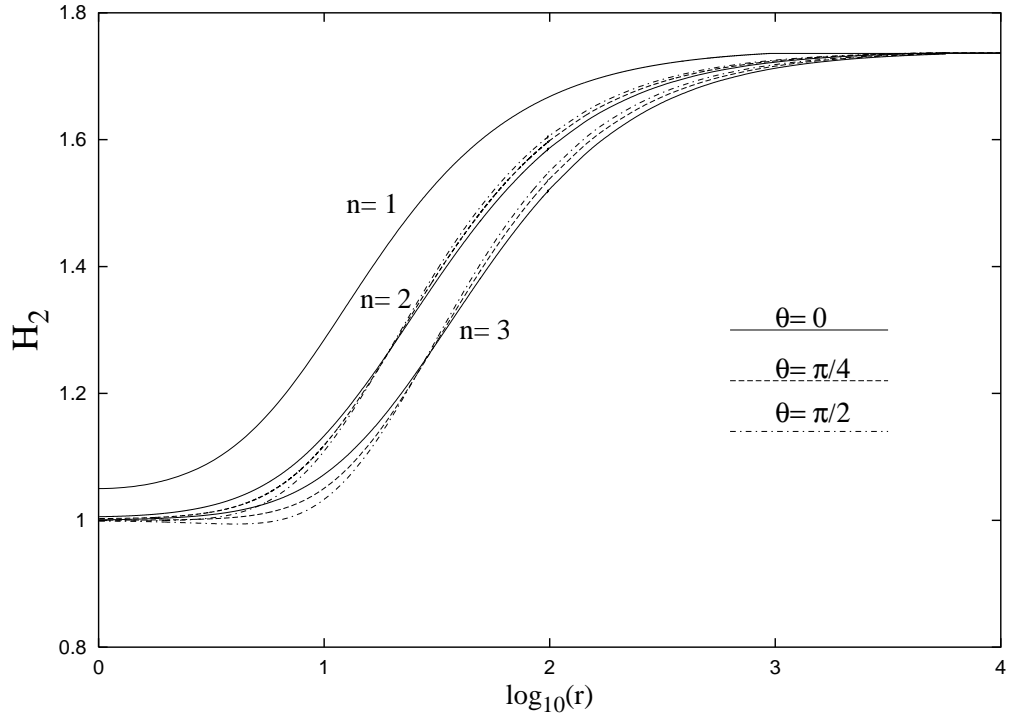
Figure 7b: Same as Fig. 7a for the gauge function H_2.

Fig. 7c
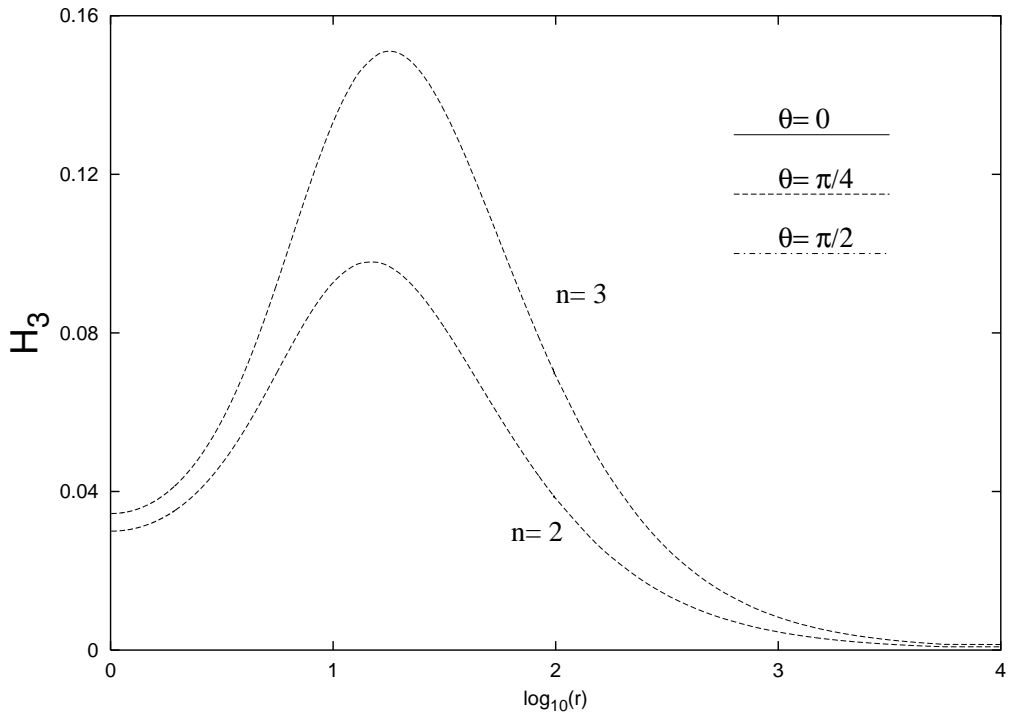
Figure 7c: Same as Fig. 7a for the gauge function H_3.

38

Fig. 7d

Figure 7d: Same as Fig. 7a for the gauge function H_4.

Fig. 7e
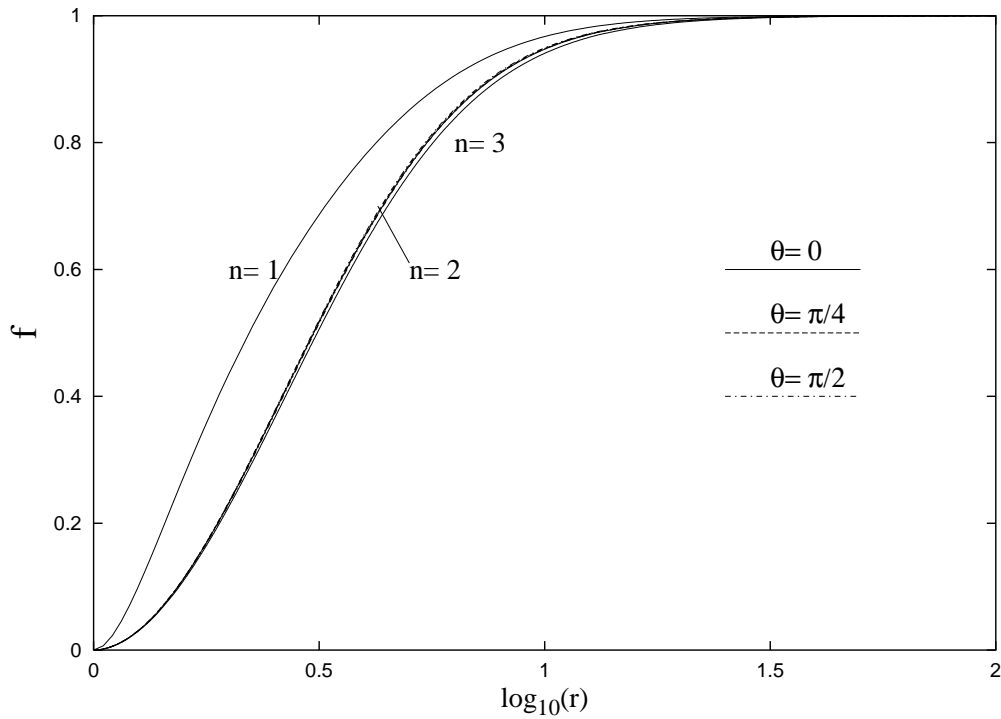
Figure 7e: Same as Fig. 7a for the metric function f.

39
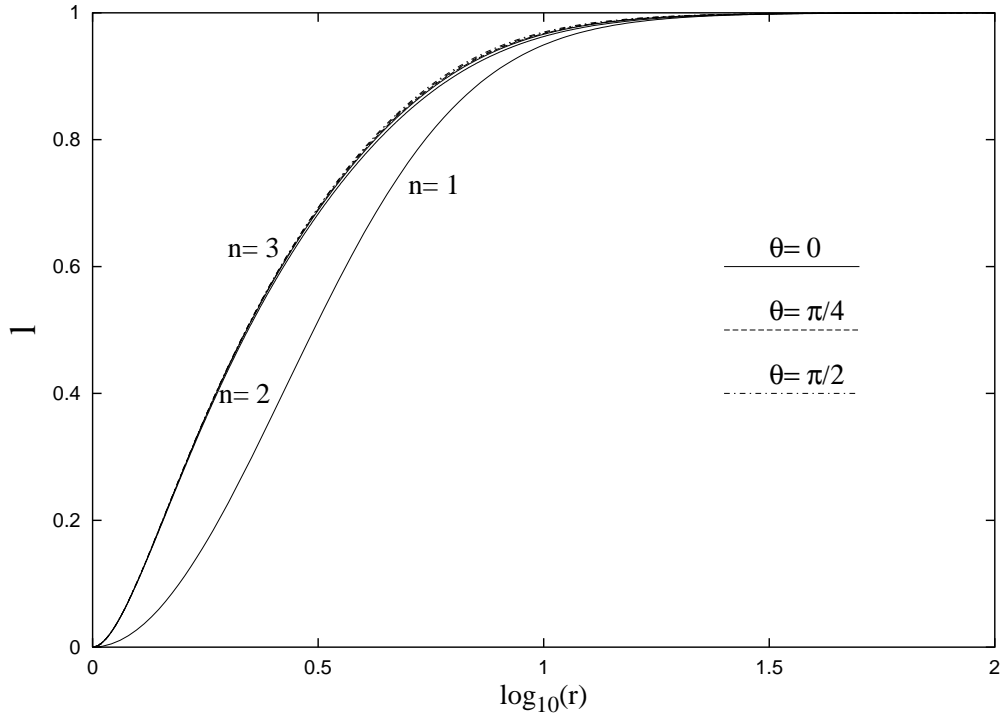
Fig. 7f

Figure 7f: Same as Fig. 7a for the metric function l.

Fig. 7e
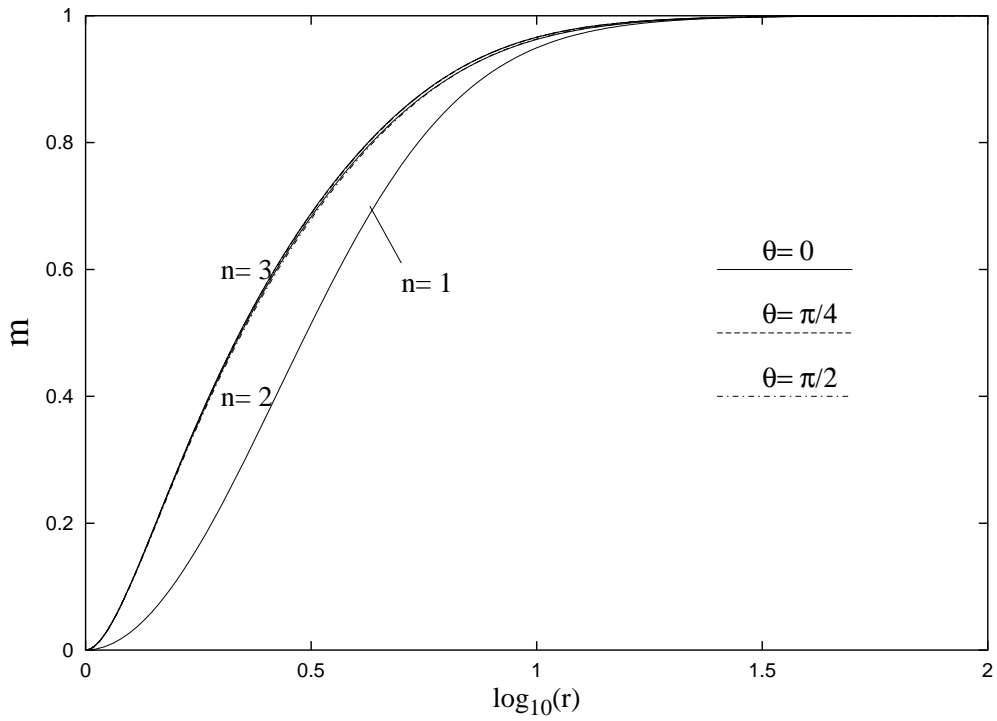
Figure 7g: Same as Fig. 7a for the metric function m.

40

Fig. 7f

Figure 7h: Same as Fig. 7a for the energy density $\epsilon = -T_t^t$ of the solutions.

Fig. 8
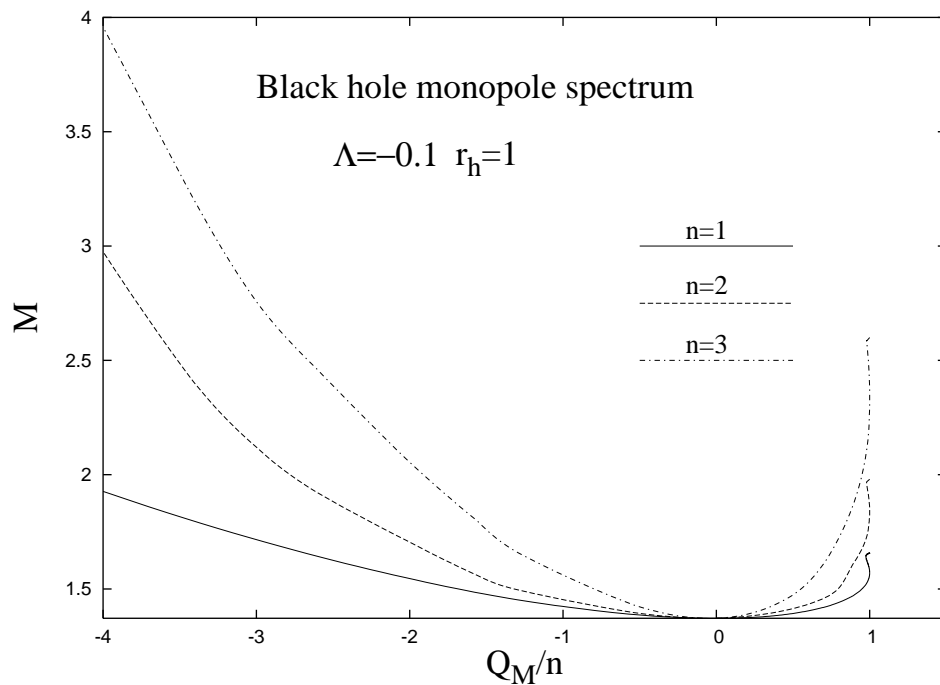
Figure 8: The total mass M is plotted as a function of magnetic charge Q_M for black hole gravitating monopole solutions at $\Lambda = -0.1$, $r_h = 1$. The winding number n is also marked.
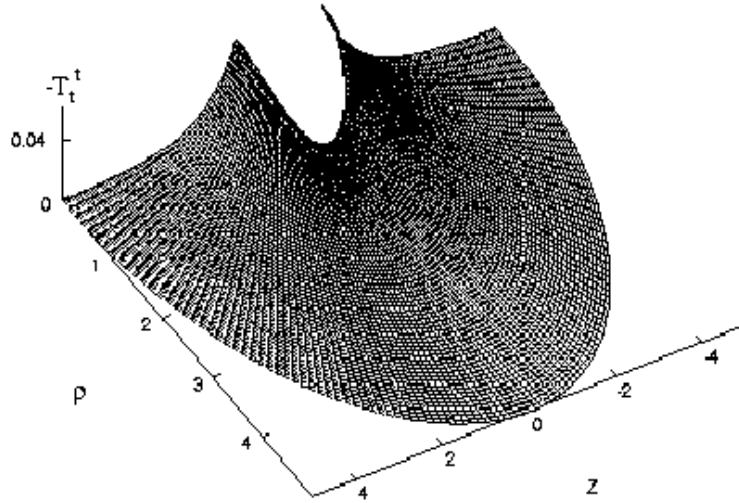
Figure 9a: The energy density $\epsilon = -T_t^t$ is shown as for a gravitating monopole solution with $\omega_0 = 0.49$, $n = 2$. Here the cosmological constant is $\Lambda = -1$ and the black hole radius is $r_h = 1$.

Fig. 9b
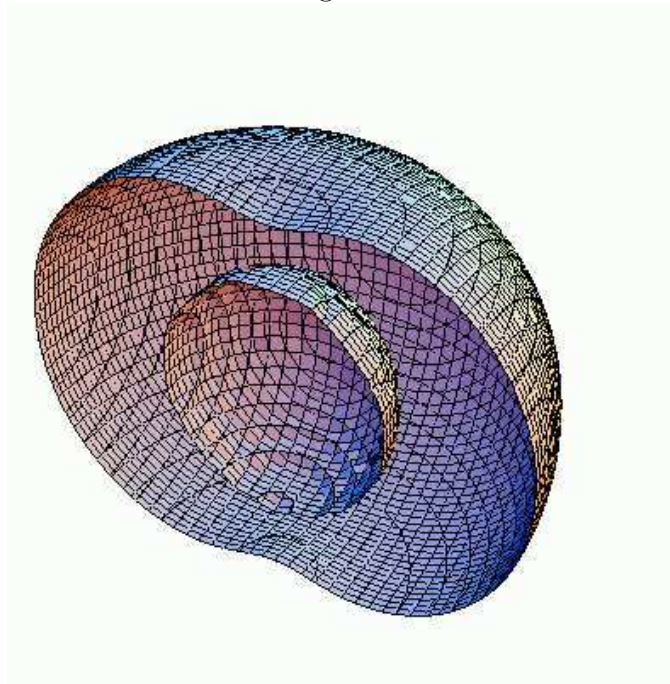
Figure 9b: A surface of constant energy density $\epsilon = -T_t^t = 0.014$ are plotted for the solution of Fig. 9a.

Fig. 9c
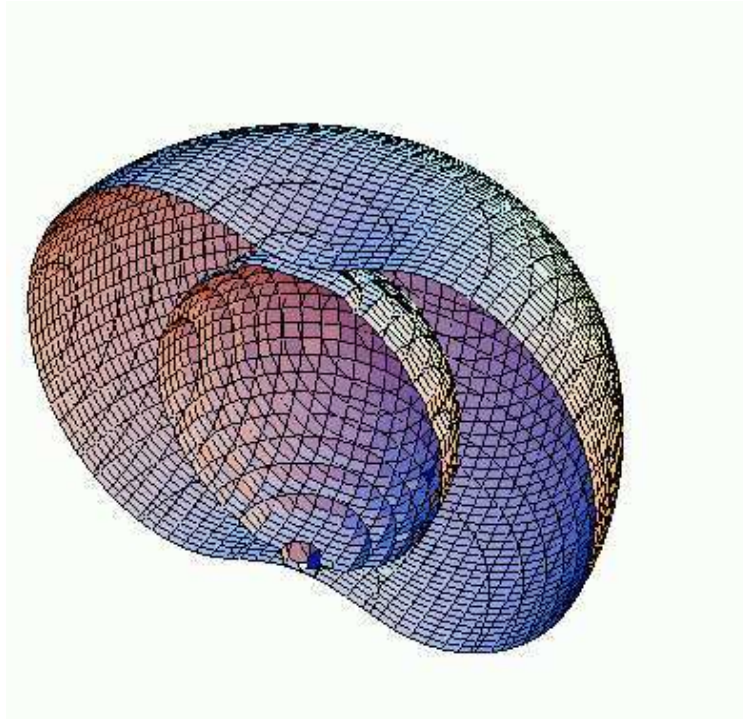
Figure 9c: Same as Fig. 9b for $\epsilon = 0.019$

Fig. 9d

Figure 9d: Same as Fig. 9b for $\epsilon = 0.03$

Figure 10a: The gauge function H_i is shown as a function of the radial coordinate r for the angles $\theta = 0$, $\pi/4$ and $\pi/2$. The results correspond to EYM black hole solutions with winding number $n = 2$, magnetic charge $Q_M = 1.52$, horizon radius $r_h = 1$ and cosmological constants $\Lambda = -1$, -0.1 and -0.001.

Fig. 10b
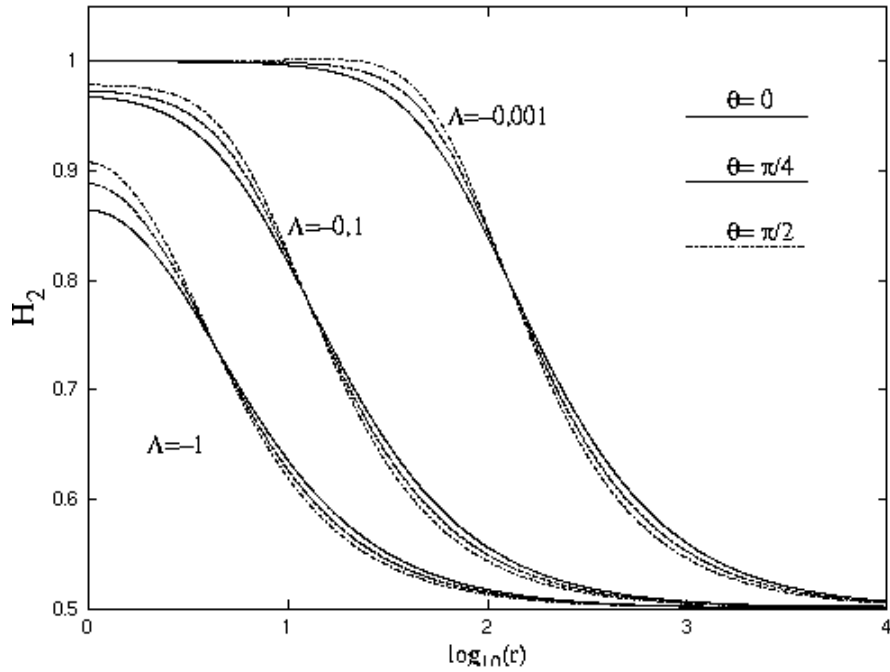
Figure 10b: Same as Fig. 10a for the gauge function H_2.
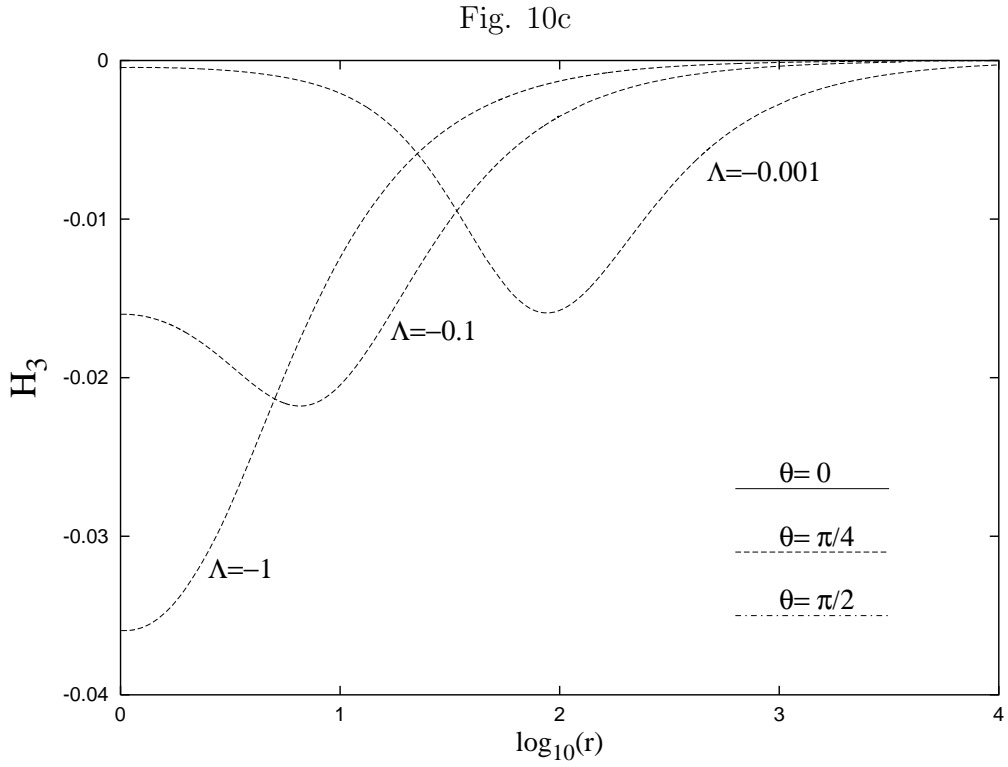
Figure 10c: Same as Fig. 10a for the gauge function H_3.
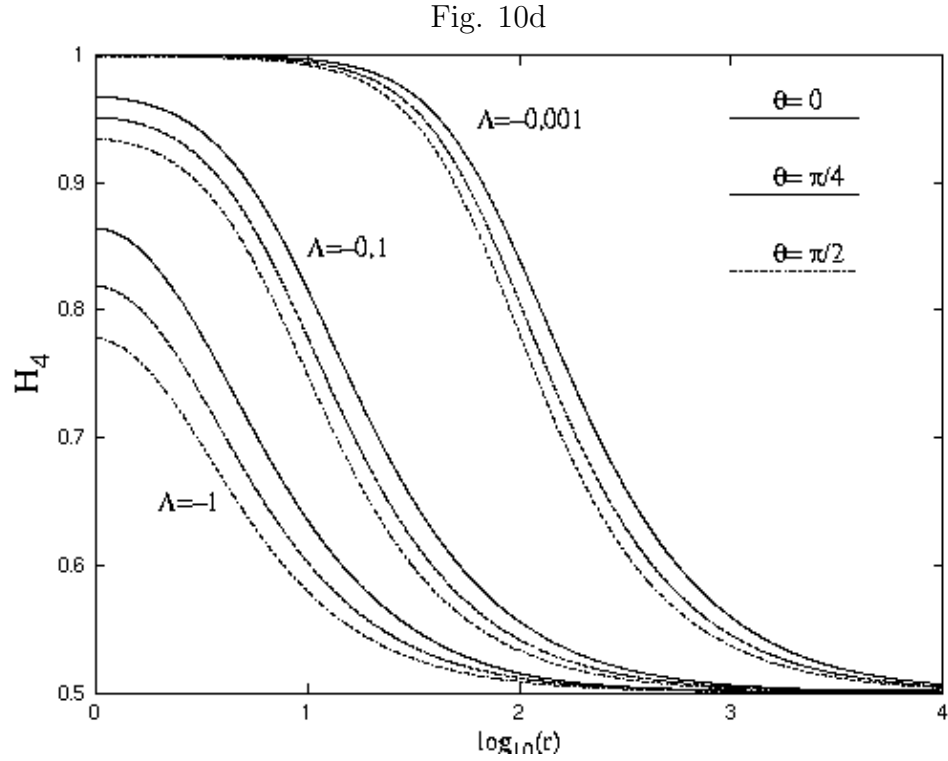
Figure 10d: Same as Fig. 10a for the gauge function H_4.

Fig. 10e
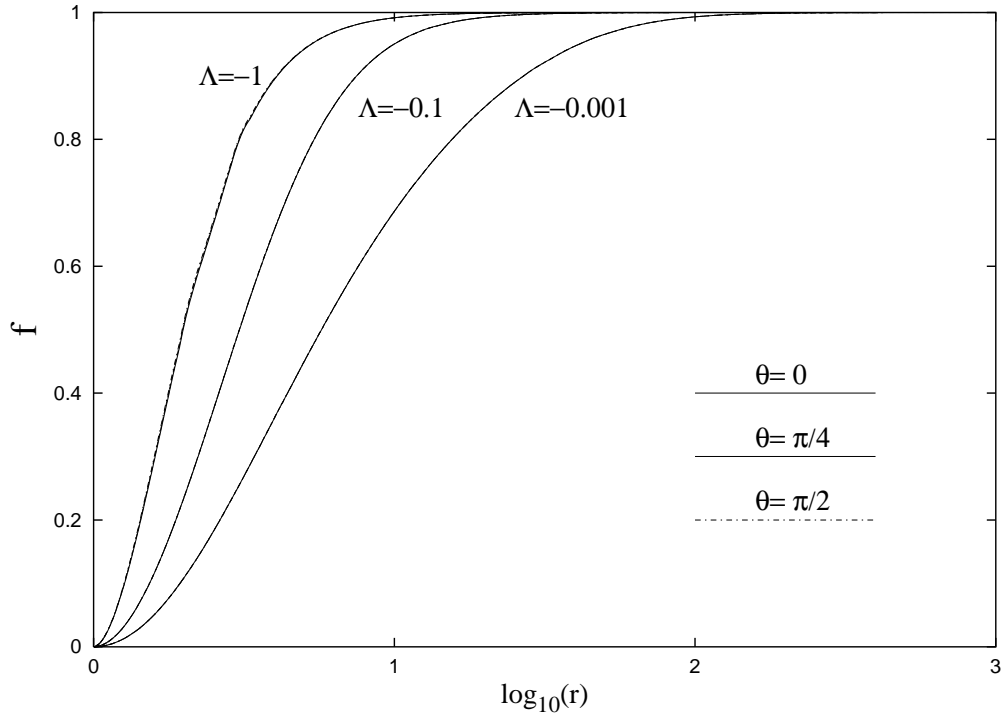
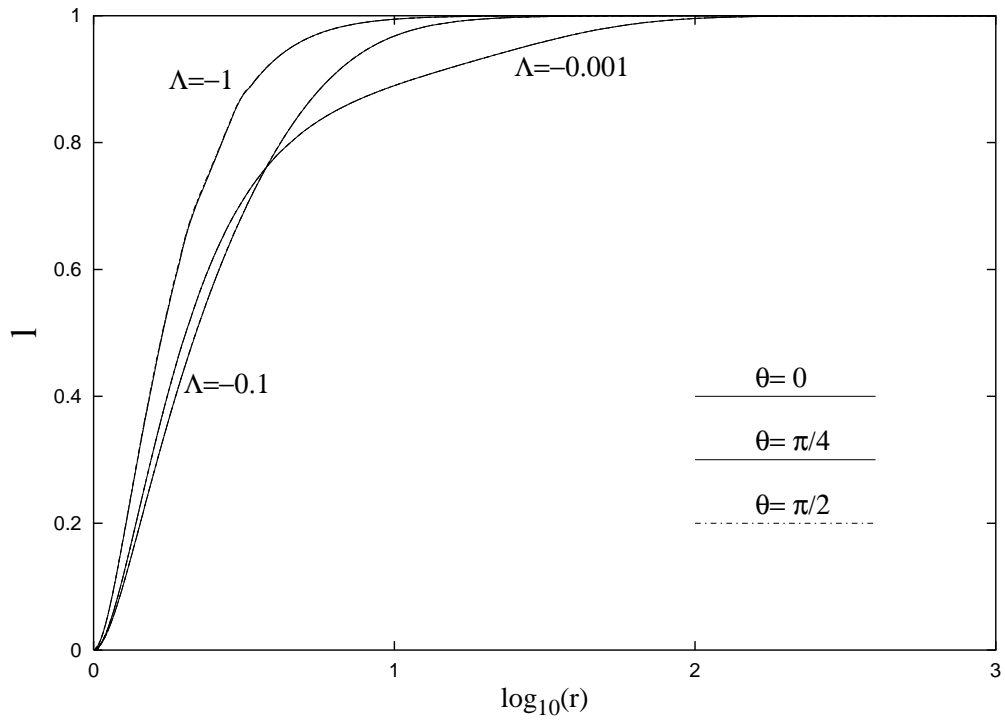Figure 10e: Same as Fig. 10a for the metric function f.

Fig. 10f

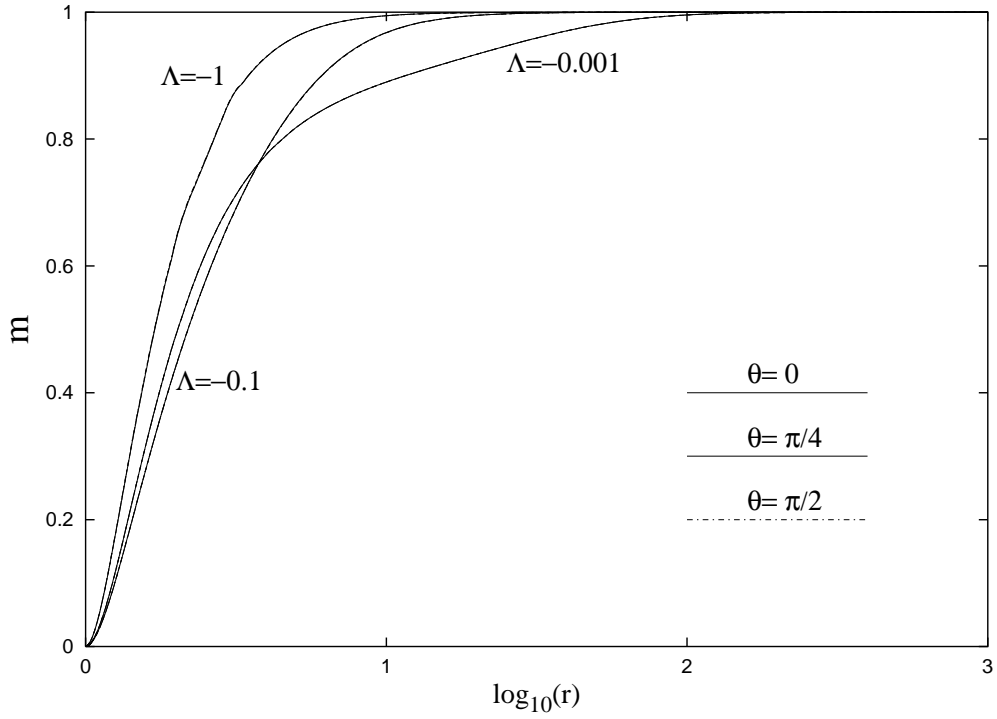Figure 10f: Same as Fig. 10a for the metric function l.

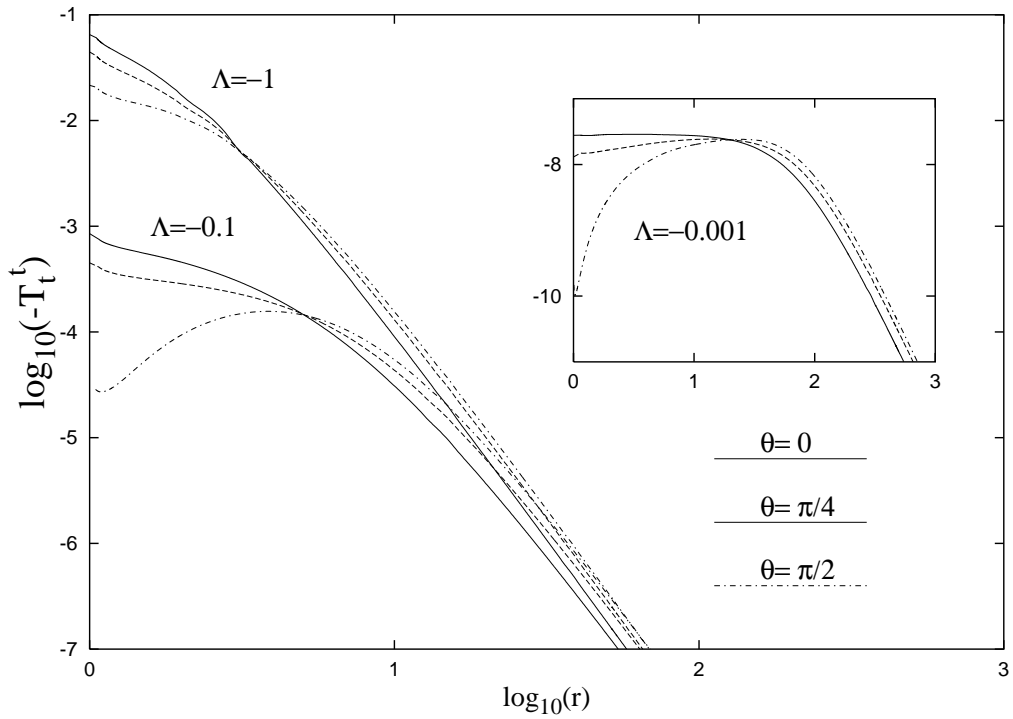Figure 10g: Same as Fig. 10a for the metric function m.

Figure 10h: Same as Fig. 10a for the energy density $\epsilon = -T^t_t$.

Fig. 11
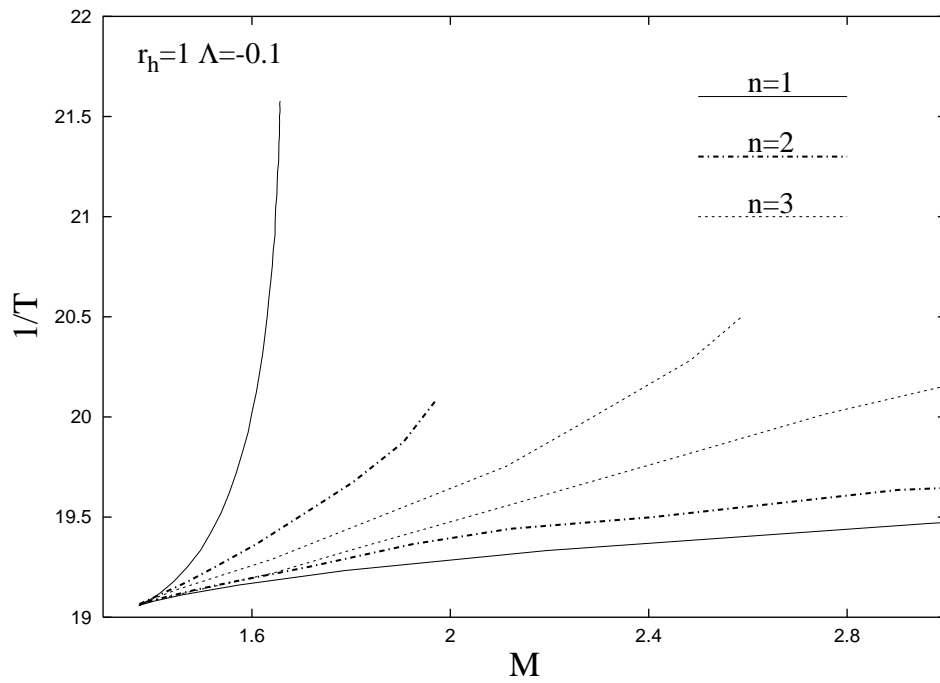
Figure 11: The mass-temperature diagrams for black hole monopole solutions at $\Lambda = -0.1$, $r_h = 1$ and three winding numbers. The value of the magnetic potential at infinity is the control parameter which varies along each curve.